XVI

The electroweak sector

Early studies of the weak interactions were confined to processes, like nuclear beta decay and muon decay, which concern just the charged weak current. Starting from the mid-1970s, the field of weak interaction phenomenology was broadened by experiments involving neutral weak currents. The advent of collider experiments made possible direct studies of the $W^{\pm}$ and Z^0 gauge bosons themselves. This chapter will first address the topic of low-energy neutral-current phenomenology and then consider physical processes at the higher mass scales M_W and M_Z. To conclude, we turn to the more theoretical topic of electroweak radiative corrections and renormalization. Throughout, we shall keep our treatment at a relatively simple introductory level.

XVI–1 Neutral weak phenomena at low energy

The words '*low energy*' in the title of this section denote processes with $Q^2 \ll M_Z^2$. We shall focus on three of these:

(1) deep-inelastic neutrino scattering (DIνS),
(2) atomic parity violation (APV),
(3) parity-violating (PV) Møller scattering.

In each case, the main finding is a determination of the weak mixing angle at the kinematical scale $\mu = Q$ appropriate to that experiment. In this context, it is convenient to use a scale-dependent version of the weak mixing angle, such as the $\overline{\rm MS}$ quantity $\hat{s}^2_{\rm w}(\mu)$.[1] Then, we display in Fig. XVI–1 the dependence of $\hat{s}^2_{\rm w}$ on Q^2 found from both low-energy and high-energy studies. Fig. XVI–1, although not yet reaching the iconic status of Fig. II–6 (which displays the asymptotic freedom

[1] We employ the common abbreviations $s_{\rm w} \equiv \sin\theta_{\rm w}$, $c_{\rm w} \equiv \cos\theta_{\rm w}$ and also employ $\hat{s}_{\rm w}$ for $\overline{\rm MS}$ renormalization. For convenience, we shall refer (admittedly loosely) to the quantity $s^2_{\rm w}$ as the 'weak mixing angle'.

https://doi.org/10.1017/9781009291033.017 Published online by Cambridge University Press

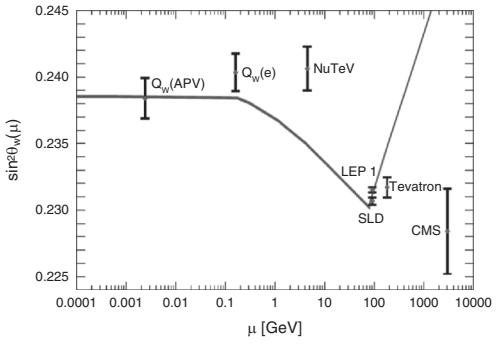

Fig. XVI–1 Scale dependence of $\hat{s}^2_{\rm w}$, from [RPP 12] (used with permission).

property of *QCD*), has become an apt representation of this field. It has, indeed, been a major achievement of low-energy neutral-current studies to verify (within experimental uncertainties) the variation of $\hat{s}^2_{\rm w}(\mu)$ with scale μ expected from the Standard Model.

One can use the renormalization group to 'run' each of the low-energy determinations up to a standard reference scale, say $\mu = M_Z$, to provide the values for $\hat{s}^2_{\rm w}(M_Z)$ shown in Table XVI–1 [KuMMS 13]. For comparison's sake is also included the quantity $\hat{s}^2_{\rm w}(M_Z)$ obtained by using an average of data from experiments carried out directly at the Z^0 scale, e.g., Z^0 decays and cross-section asymmetries, cf. Sect. XVI–2. At present, the high-energy determination is far more accurate than the low-energy determination due to its dominance in statistics.

Neutral-current effective lagrangians

To provide a theoretical language for such low-energy experiments, let us identify effective lagrangians for some neutral-current processes. Recall from Eq. (II–3.40) that the neutral weak interaction between the gauge boson Z^0 and a fermion f is given at tree level by

Table XVI–1. *Weak mixing angle from neutral-current experiments*

Experiment	$\langle Q^2 \rangle (\mathrm{GeV}^2)$	$\hat{s}^2_{\rm w}(M_Z)$
DIνS	20	0.2356(16)
APV (in Cs)	5.8×10^{-6}	0.2383(20)
PV Møller	2.6×10^{-2}	0.2329(13)
Average at Z mass scale	$M_Z^2 \simeq 8.3 \times 10^3$	0.23125(016)

https://doi.org/10.1017/9781009291033.017 Published online by Cambridge University Press

$$\mathcal{L}^{(f)}_{\text{ntl}-\text{wk}} = -\frac{g_{2,0}}{2c_{\text{w},0}}\, Z_\mu\, \bar{f}\left(g^{(f)}_{\text{v},0}\gamma^\mu + g^{(f)}_{\text{a},0}\gamma^\mu\gamma_5\right) f$$
$$g^{(f)}_{\text{v},0} = T^{(f)}_{\text{w}3} - 2s^2_{\text{w},0}Q^{(f)}_{\text{el}}, \qquad g^{(f)}_{\text{a},0} = T^{(f)}_{\text{w}3}, \tag{1.1}$$

where we denote tree-level parameters with a '0' subscript. Examples of individual $g^{(f)}_{\text{v},0}$ and $g^{(f)}_{\text{a},0}$ appear in Eq. (II–3.41). To describe neutral-current interactions at low energies, one forms an effective four-fermion lagrangian, akin to the Fermi model of charged-current interactions. At tree level, the Z^0-mediated interaction in the low-energy limit is

$$\mathcal{L} = -\frac{1}{2}\frac{g^2_{2,0}}{4c^2_{\text{w},0}}\sum_{f,f'}\overline{f}\left(g^{(f)}_{\text{v},0}\gamma^\mu + g^{(f)}_{\text{a},0}\gamma^\mu\gamma_5\right) f\ \frac{1}{M^2_{Z,0}}\ \overline{f}'\left(g^{(f')}_{\text{v},0}\gamma_\mu + g^{(f')}_{\text{a},0}\gamma_\mu\gamma_5\right) f'$$
$$= -\rho_0\frac{G_\mu}{\sqrt{2}}\sum_{f,f'}\overline{f}\left(g^{(f)}_{\text{v},0}\gamma^\mu + g^{(f)}_{\text{a},0}\gamma^\mu\gamma_5\right) f\ \overline{f}'\left(g^{(f')}_{\text{v},0}\gamma_\mu + g^{(f')}_{\text{a},0}\gamma_\mu\gamma_5\right) f', \tag{1.2}$$

where ρ_0 is the tree-level *rho parameter*,

$$\rho_0 \equiv \frac{1}{c^2_{\text{w},0}}\frac{M^2_{W,0}}{M^2_{Z,0}}. \tag{1.3}$$

Comparison of the second of the relations in Eq. (1.2) with Eq. (V–2.1) shows that ρ_0 governs the relative strengths of the neutral and charged weak-current effective lagrangians. In the Standard Model, it has the tree-level value unity, $\rho_0^{(\text{SM})} = 1$. The reader might wonder – why include a quantity, ρ_0, whose Standard Model value is unity? There are actually two reasons: (i) although $\rho_0^{(\text{SM})} = 1$, ρ_0 is *not* unity in general, e.g., alternative choices for Higgs structure can lead to different values for ρ_0 (cf. Prob. XV–1), and (ii) even in the Standard Model, electroweak corrections will change its value away from unity (cf. Sect. XVI–6).

The set of low-energy neutral-current processes includes neutrino–electron, neutrino–quark, and parity-violating electron–quark interactions. There is an effective lagrangian for each of these, two examples being

$$\mathcal{L}_{\nu q} = -\frac{G_\mu}{\sqrt{2}}\,\overline{\nu}_\ell\gamma^\mu(1+\gamma_5)\nu_\ell\left[\epsilon^{(\alpha)}_L\overline{q}_\alpha\gamma_\mu(1+\gamma_5)q_\alpha + \epsilon^{(\alpha)}_R\overline{q}_\alpha\gamma_\mu(1-\gamma_5)q_\alpha\right]$$
$$\mathcal{L}^{(\text{p.v.})}_{\text{eq}} = -\frac{G_\mu}{\sqrt{2}}\left[C^\alpha_1\overline{e}\gamma^\mu\gamma_5 e\,\overline{q}_\alpha\gamma_\mu q_\alpha + C^\alpha_2\overline{e}\gamma^\mu e\,\overline{q}_\alpha\gamma_\mu\gamma_5 q_\alpha\right], \tag{1.4}$$

where the index $\alpha = u, d, \ldots$ denotes quark flavor. Of course, contributions other than neutral weak effects also enter, e.g., parity-conserving eq scattering experiences the electromagnetic interaction.

In Eq. (1.4), we have implicitly included the effect of radiative corrections and thus omit the subscript '0'. Table XVI–2 gives a compilation of the radiatively

https://doi.org/10.1017/9781009291033.017 Published online by Cambridge University Press

Table XVI–2. *Radiatively corrected coefficients.*

Coefficient	General form[a]
$\epsilon_L^{(u)}$	$\rho_{\nu N}\left(\frac{1}{2}-\frac{2}{3}\kappa_{\nu N}s_{\rm w}^2\right)$
$\epsilon_L^{(d)}$	$\rho_{\nu N}\left(-\frac{1}{2}+\frac{1}{3}\kappa_{\nu N}s_{\rm w}^2\right)$
$\epsilon_R^{(u)}$	$\rho_{\nu N}\left(-\frac{2}{3}\kappa_{\nu N}s_{\rm w}^2\right)$
$\epsilon_R^{(d)}$	$\rho_{\nu N}\left(\frac{1}{3}\kappa_{\nu N}s_{\rm w}^2\right)$
C_1^u	$\rho_{\rm eq}\left(-\frac{1}{2}+\frac{4}{3}\kappa_{\rm eq}s_{\rm w}^2\right)$
C_1^d	$\rho_{\rm eq}\left(\frac{1}{2}-\frac{2}{3}\kappa_{\rm eq}s_{\rm w}^2\right)$

[a] Small additive terms are omitted.

corrected coefficients (with renormalization scheme left unspecified). The quantities ρ_i and κ_i in Table XVI–2 reduce at tree level to unity, $\rho_{i,0}=\kappa_{i,0}=1$. The ρ_i are overall multiplicative factors and the κ_i multiply the weak mixing angle, which itself has become renormalized, $s^2_{\rm w,0}\to s^2_{\rm w}$. The presence of such quantities in the effective lagrangians can be traced back to the underlying neutral-current couplings,

$$g_{\rm v,0}^{(f)}\to g_{\rm v}^{(f)}=\sqrt{\rho_f}\left(T_{\rm w3}^{(f)}-2\kappa_f s_{\rm w}^2 Q_{\rm el}^{(f)}\right),\qquad g_{\rm a,0}^{(f)}\to g_{\rm a}^{(f)}=\sqrt{\rho_f}\,T_{\rm w3}^{(f)},\quad (1.5)$$

where, again, we leave the renormalization scheme unspecified. However, see [MaS 80] for the introduction of $\overline{\rm MS}$ renormalization to electroweak corrections. The quantities ρ_i and κ_i will be discussed in more detail later in Sect. XVI–6.

Deep-inelastic neutrino scattering from isoscalar targets

In deep-inelastic scattering, one measures the ratios of neutral to charged-current neutrino/antineutrino cross sections,

$$R_\nu\equiv\sigma_{\nu N}^{\rm NC}/\sigma_{\nu N}^{\rm CC},\qquad R_{\bar\nu}\equiv\sigma_{\bar\nu N}^{\rm NC}/\sigma_{\bar\nu N}^{\rm CC}.\quad (1.6)$$

Under the conditions of 'deep-inelastic' kinematics ([BaP 87]), theoretical calculations of R_ν and $R_{\bar\nu}$ are carried out in terms of quark, rather than hadronic, degrees of freedom. It is plausible that by working with *ratios* like those in Eq. (1.6), theoretical uncertainites associated with hadron structure tend to cancel. At tree level, R_ν and $R_{\bar\nu}$ are straightforwardly computed if scattering from an isoscalar target is assumed and antiquark contributions are ignored. It is useful to express the $\epsilon_{L,R}^{(\alpha)}$ coefficients of Eq. (1.4) as

https://doi.org/10.1017/9781009291033.017 Published online by Cambridge University Press

$$g_L^2 \equiv \left(\epsilon_L^{(u)}\right)^2 + \left(\epsilon_L^{(d)}\right)^2 \simeq \frac{1}{2} - s_{\mathrm{w},0}^2 + \frac{5}{9}\left(1 + r_0\right) s_{\mathrm{w},0}^4,$$
$$g_R^2 \equiv \left(\epsilon_R^{(u)}\right)^2 + \left(\epsilon_R^{(d)}\right)^2 \simeq \frac{5}{9} s_{\mathrm{w},0}^4. \tag{1.7}$$

These quantities can be determined from the combination of neutrino and anti-neutrino cross sections,

$$R_\pm \equiv \frac{R_\nu \pm r R_{\bar{\nu}}}{1 \pm r} = g_L^2 \pm g_R^2, \tag{1.8}$$

where $r = 1/\bar{r} \equiv \sigma_{\bar{\nu}N}^{\mathrm{CC}}/\sigma_{\nu N}^{\mathrm{CC}}$ are measurable quantities with tree-level values $r_0 = \bar{r}_0^{-1} = 3$. The NuTeV experiment [Ze *et al*. 01] at Fermilab, carried out at an average momentum-squared transfer $\langle Q^2 \rangle = \langle -q^2 \rangle \simeq 20$ GeV^2, has yielded the most precise determination to date,

$$g_L^2 = 0.3005 \pm 0.0014, \quad g_R^2 = 0.0310 \pm 0.0011. \tag{1.9}$$

This translates into a determination of the weak mixing angle, which lies nearly 3σ above the stated Standard Model prediction, a finding which has spurred much discussion since then.

Atomic parity violation in cesium

The Z^0-mediated electron–nucleus interaction, expressed here in the electron spin space, contains a component which is parity-violating,

$$\mathcal{H}_{\mathrm{PNC}}(r) = \frac{G_\mu}{2\sqrt{2}} Q_{\mathrm{w}} \gamma_5 \rho_{\mathrm{nucl}}(r), \tag{1.10}$$

where γ_5 signals the presence of parity violation and $\rho_{\mathrm{nucl}}(r)$ reminds us that the electron feels the effect only where the nuclear density is nonvanishing.[2] The quantity Q_{w} is the 'weak nuclear charge' to which the electron couples, and is given to lowest order by

$$Q_{\mathrm{w},0}(N, Z) = -2\left(N_u C_{1,0}^u + N_d C_{1,0}^d\right) = Z\left(1 - 4 s_{\mathrm{w},0}^2\right) + N, \tag{1.11}$$

where Z and N are, respectively, the nuclear proton and neutron number. The fact that $s_{\mathrm{w},0}^2 \simeq 0.25$ suppresses the proton contribution, leaving the coupling of the atomic electron to neutrons as dominant.

Consider the effect in atomic cesium, ^{138}Ce. Because of the neutral weak-current interaction, the single valence electron in cesium contains small admixtures of P wave in its $6S$ (ground) and $7S$ (excited) states. We write these mixed states as $|\overline{6S}\rangle$

[2] The abbreviation 'PNC' stands for *parity nonconservation*.

https://doi.org/10.1017/9781009291033.017 Published online by Cambridge University Press

and $|\overline{7S}\rangle$. As a consequence, there occurs a measurable parity-violating $7S \to 6S$ electric-dipole (E1) transition matrix element [NoMW 88],

$$\mathcal{I}m\ E_{\rm PNC} = \langle \overline{7S}|\mathbf{D}|\overline{6S}\rangle \equiv \frac{Q_{\rm w}}{N} k_{\rm PNC}, \tag{1.12a}$$

where $\mathbf{D}$ is the electric-dipole operator and

$$k_{\rm PNC} \equiv \frac{N}{Q_{\rm w}} \sum_n \left[\frac{\langle 7S|\mathbf{D}|nP\rangle\langle nP|H_{\rm PNC}|6S\rangle}{E_{6S} - E_{nP}} + \frac{\langle 7S|H_{\rm PNC}|nP\rangle\langle nP|\mathbf{D}|6S\rangle}{E_{7S} - E_{nP}} \right]. \tag{1.12b}$$

The experiments involve finding the ratio of the PNC amplitude $E_{\rm PNC}$ to the vector transition probability β. The most accurate results to date on the $6S \to 7S$ transition are $E_{\rm PNC}/\beta = 1.5935(56)$ mV cm^{-1} [BeCMRTWW 97] and $\beta = 26.957(51)\ a_{\rm B}^3$ [BeW 99]. However, interpretation of the PNC measurements requires evaluating Eq. (1.12b) and this contains intractable aspects of the atomic many-body problem. There has, however, been recent progress [PoBD 09] and the latest calculation gives [DzBFR 12] $E_{\rm PNC} = 0.08977(40)i(-Q_{\rm w}/N)$, implying the weak-charge value

$$Q_{\rm w}(^{138}{\rm Ce}) = -72.58(29)_{\rm expt}(32)_{\rm thy}, \tag{1.13}$$

where the uncertainties refer respectively to statistical and theoretical contributions. This result lies about 1.5σ beneath the Standard Model prediction $Q_{\rm w}^{\rm (SM)}(^{138}{\rm Ce}) = -73.23(2)$.

Polarized Møller scattering

Another experiment which has probed the weak mixing angle at a low-energy scale is polarized Møller scattering [An *et al.* (SLAC E158 collab.) 05], where we remind the reader that Møller scattering is the elastic scattering of electrons on electrons. In SLAC E158, a 50 GeV beam of longitudinally polarized electrons was scattered from an unpolarized fixed target. The parity-violating observable is the asymmetry

$$A_{\rm pv} = \frac{\sigma_R - \sigma_L}{\sigma_R + \sigma_L}, \tag{1.14}$$

where $\sigma_{R(L)}$ is the cross section for incident right (left) polarized electrons. Relevant kinematic variables are the center-of-mass-squared energy $s = (p + p')^2$, the momentum transfer $Q^2 = -q^2 = -(p - p')^2$, and the ratio of the two, $y \equiv Q^2/s = (1 - \cos\theta)/2$, where θ is the scattering angle in the center of mass. The experiment was carried out with average values $\langle Q^2\rangle = 0.026$ GeV^2 and $\langle y\rangle \simeq 0.6$; the tiny asymmetry $A_{\rm pv} = -131(14)_{\rm stat}(10)_{\rm sys} \times 10^{-9}$ was found.

https://doi.org/10.1017/9781009291033.017 Published online by Cambridge University Press

There are three parts to the theory analysis. First is the tree-level amplitude, where the Møller scattering amplitude arises from t-channel and u-channel γ and Z^0 exchange diagrams. Parity violation is due to the interference of the electromagnetic and weak neutral-current amplitudes. An approximate tree-level expression for $A_{\rm pv}$ which is valid for the conditions of the E158 experiment is

$$A_{\rm pv}^{(\rm tree)} \simeq \frac{G_\mu Q^2}{\sqrt{2}\pi\alpha} \cdot \frac{1-y}{1+y^4+(1-y)^4} \left(1 - 4\sin^2\theta_{\rm w,0}\right). \tag{1.15}$$

The dependence on the weak mixing angle suppresses $A_{\rm pv}^{(\rm tree)}$ due to the proximity of $\sin^2\theta_{\rm w,0}$ to $1/4$.

Next are the one-loop corrections, due mainly to the γ–Z^0 propagator-mixing terms induced by fermion and W-boson loop amplitudes [CzM 96]. These are absorbed by the $\overline{\rm MS}$ running weak mixing angle,

$$\hat{s}^2_{\rm w}(\mu) = (1 + \Delta\kappa(\mu))\, \hat{s}^2_{\rm w}(M_Z), \tag{1.16a}$$

as parameterized by $\Delta\kappa(\mu)$. In particular, one finds $\Delta\kappa(0) \simeq 0.03$, so that

$$1 - 4\sin\theta^2_{\rm w} \simeq 0.075 \implies 1 - \kappa(0)\hat{s}^2_{\rm w}(M_Z) \simeq 0.046. \tag{1.16b}$$

The rather small ($\sim$3%) effect of $\Delta\kappa(0)$ translates into a major ($\sim$40%) change in $1 - 4\sin\theta^2_{\rm w}$! Finally comes the renormalization-group-improved analysis [ErR-M 05]. This serves to ameliorate the dependence on large logarithms ($\ln(m_f^2/Q^2)$ and $\ln(M_W^2/Q^2)$ for fermion and W-boson loops respectively), which appear in the one-loop amplitudes. This results in the improved determinations,

$$\Delta\kappa(0) = 0.03232 \pm 0.00029, \qquad \hat{s}^2_{\rm w}(0) = 0.23867 \pm 0.00016. \tag{1.17}$$

XVI–2 Measurements at the Z^0 mass scale

The collection of resonances observed in $e\bar{e}$ collisions as a function of the total center-of-mass energy is displayed in Fig. XVI–2. At the Z^0 mass scale, it is the *weak* interaction which dominates the physics in this reaction, with strong and electromagnetic effects merely supplying modest corrections. An enormous database has been established at the Z^0 factories with the LEP1 experiments at CERN and the SLD collaboration at SLAC. There also exists data from $p\bar{p} \to f^+f^-$ measured at the Tevatron as well as that from $pp \to \ell^+\ell^- + X$ taken by the LHC detectors. These experiments have come to be analyzed in terms of a so-called 'effective description' wherein the renormalized vector and axial-vector couplings of Eq. (1.5) are written as

$$\bar{g}_{\rm v}^{(f)} = \sqrt{\rho_f}\left(T_{\rm w3}^{(f)} - 2\bar{s}_f^2 Q_{\rm el}^{(f)}\right), \qquad \bar{g}_{\rm a}^{(f)} = \sqrt{\rho_f}\, T_{\rm w3}^{(f)}, \tag{2.1}$$

https://doi.org/10.1017/9781009291033.017 Published online by Cambridge University Press

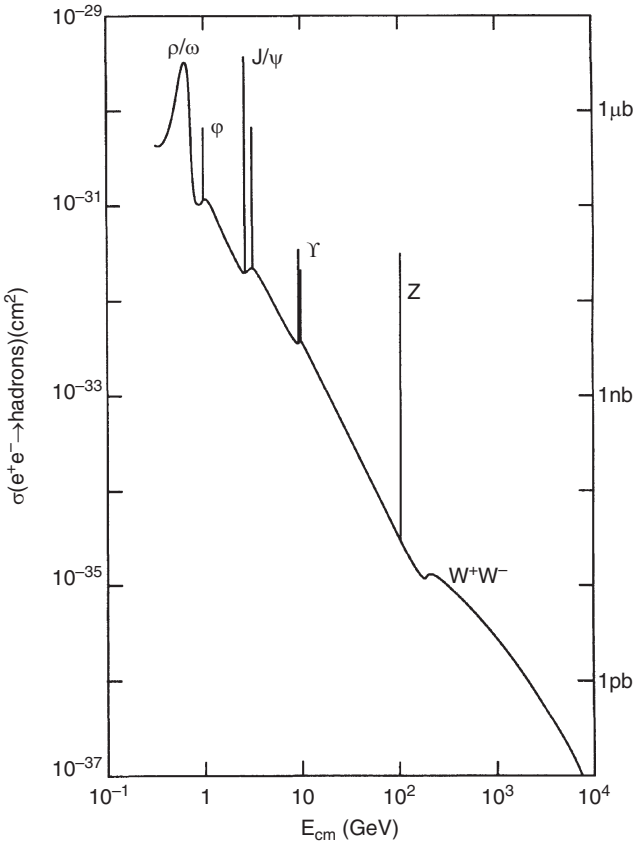

Fig. XVI–2 Resonances in $e\bar{e}$ collisions.

where the superbars denote evaluation in the effective renormalization scheme associated with the scale $\mu = M_Z$. In this approach, the effective weak mixing angle $\bar{s}_f$ for fermion f is defined so as to absorb the κ_f factor in Eq. (1.5) [Sc *et al.* 06],

$$\bar{s}_f^2 \equiv \kappa_f s_{\rm w}^2, \tag{2.2a}$$

and can be measured experimentally by

$$\bar{s}_f^2 = \frac{1}{4}\left(1 - \bar{g}_{\rm v}^{(f)}/\bar{g}_{\rm a}^{(f)}\right), \tag{2.2b}$$

independent of the quantity κ_f.[3]

We shall discuss two kinds of measurements in the following: Z^0 decay into fermion–antifermion pairs, which is sensitive to $(\bar{g}_{\rm v}^{(f)})^2 + (\bar{g}_{\rm a}^{(f)})^2$, and cross-section

[3] Although both ρ_f and κ_f are both generally *complex-valued*, we shall tacitly use just the real part without further comment.

https://doi.org/10.1017/9781009291033.017 Published online by Cambridge University Press

asymmetries in the reaction $e^- e^+ \to f\bar{f}$ at energy $\sqrt{s} = M_Z$, which determine the ratios $\bar{g}_{\rm v}^{(f)}/\bar{g}_{\rm a}^{(f)}$ and thus lead to precise determinations of $\bar{s}_f^2$ but not of the individual couplings themselves. However, between the two kinds of experiments a full determination of the couplings becomes possible. A comprehensive review of Z^0-related studies carried out at CERN and SLAC appears in [Sc *et al*. 06].

Decays of Z^0 into fermion–antifermion pairs

Experiments at the LEP and SLD colliders have provided accurate determinations of the Z^0 mass and decay modes [Sc *et al*. 06]. To lowest order, the decay of a Z^0 boson into a fermion–antifermion pair $f\bar{f}$ can be conveniently expressed as

$$\mathcal{L}_{\rm ntl}^{(f\bar{f})} = \left(\sqrt{2} G_\mu M_Z^2\right)^{1/2} Z^\mu \bar{f} \gamma_\mu \left(g_{\rm v}^{(f)} + g_{\rm a}^{(f)} \gamma_5\right) f, \tag{2.3}$$

where $f = u, d, \nu_e, e, \ldots$. Upon defining $y \equiv m^2/M_Z^2$ for fermion mass m, we obtain for the lowest-order transition rate to a pair $f\bar{f}$,

$$\Gamma_{Z^0 \to f\bar{f}}^{(0)} = \frac{N_c}{6\pi} \frac{G_\mu M_Z^3}{\sqrt{2}} \left(g_{\rm v}^{(f)2} + g_{\rm a}^{(f)2}\right) \sqrt{1-4y} \left[1 + 2y \frac{g_{\rm v}^{(f)2} - 2g_{\rm a}^{(f)2}}{g_{\rm v}^{(f)2} + g_{\rm a}^{(f)2}}\right]$$
$$\xrightarrow[y \to 0]{} \frac{N_c}{6\pi} \frac{G_\mu M_Z^3}{\sqrt{2}} \left(g_{\rm v}^{(f)2} + g_{\rm a}^{(f)2}\right), \tag{2.4a}$$

where $N_c = 3$ if f is a quark and unity otherwise. If the final-state fermions are quarks, *QCD*-radiative corrections modify Eq. (2.4a) by a multiplicative factor δ_{QCD},

$$\delta_{QCD} = 1 + \frac{\alpha_s\left(M_W^2\right)}{\pi} + 1.41 \left(\frac{\alpha_s(M_W^2)}{\pi}\right)^2 + \cdots \simeq 1.04, \tag{2.4b}$$

where $\alpha_s(M_W^2) \simeq 0.12$ has been used in the above.

There exist also electroweak radiative effects, which we can take into account by employing the effective weak coupling constants $\bar{g}_{\rm v}^{(f)}$ and $\bar{g}_{\rm a}^{(f)}$ of Eq. (2.1). Upon including both strong and electroweak corrections, the tree-level relation of Eq. (2.4a) is replaced (shown here in the limit of massless final-state fermions) by

$$\Gamma_{Z^0 \to f\bar{f}} = \eta_f \frac{N_c}{6\pi} \frac{G_\mu M_Z^3}{\sqrt{2}} \left(\bar{g}_{\rm v}^{(f)2} + \bar{g}_{\rm a}^{(f)2}\right), \tag{2.5}$$

where $\eta_f = \delta_{QCD}$ if f is a quark and $\eta_f = 1$ otherwise.

Some Z^0 decay-related quantities are listed in Table XVI–3. These results are taken from [Sc *et al*. 06], but many others are provided in this source. Although there will be some adjustments from more recent studies (e.g. see [RPP 12]), the overall picture provided by [Sc *et al*. 06] bears testimony to an impressive advance

https://doi.org/10.1017/9781009291033.017 Published online by Cambridge University Press

Table XVI–3. Z^0 *decay [Sc et al. 06].*

Measurable[a]	Experiment	Standard Model prediction
$\Gamma_{e\bar{e}}$	83.9 ± 0.1	84.00 ± 0.01
$\Gamma_{\rm inv}$	496.2 ± 8.8	501.66 ± 0.03
$\Gamma_{b\bar{b}}$	377.3 ± 0.3	375.98 ± 0.03
$\Gamma_{\rm tot}$	2495.2 ± 2.3	2496.0 ± 0.2
$\bar{g}_{\rm v}^{(\ell)2}$	0.0012 ± 0.0003	$0.0011 \to 0.0013$
$\bar{g}_{\rm a}^{(\ell)2}$	0.2492 ± 0.0012	$0.2513 \to 0.2518$

[a] Decay widths are expressed in units of MeV.

in particle physics. One application, among many, of the Z^0 decays is to use leptonic modes to test the concept of lepton universality, and one finds

$$\frac{\Gamma_{\mu\bar{\mu}}}{\Gamma_{e\bar{e}}} = 1.0009 \pm 0.0027, \qquad \frac{\Gamma_{\tau\bar{\tau}}}{\Gamma_{e\bar{e}}} = 1.0021 \pm 0.0030, \tag{2.6}$$

which is seen to be consistent with universality.

Asymmetries at the Z^0 peak

For the reaction $e^- e^+ \to f\bar{f}$ carried out at the Z^0 peak a natural variable is the *asymmetry parameter* for fermion f,

$$\mathcal{A}_f \equiv 2\frac{\bar{g}_{\rm v}^{(f)}\bar{g}_{\rm a}^{(f)}}{\bar{g}_{\rm v}^{(f)2} + \bar{g}_{\rm a}^{(f)2}} = 2\frac{\bar{g}_{\rm v}^{(f)}/\bar{g}_{\rm a}^{(f)}}{1 + \left(\bar{g}_{\rm v}^{(f)2}/\bar{g}_{\rm a}^{(f)2}\right)}, \tag{2.7}$$

which can be determined experimentally from angular distribution and/or polarization data, as discussed below. In the case that the final-state fermion f is a quark q, then it is hadrons which are detected and the final-state hadronic charge asymmetry which is measured. It is to be understood that the measured data have been corrected for contributions such as initial-state *QED* corrections, γ exchange, γ–Z^0 interference, etc., leaving asymmetries which are purely electroweak in origin. Finally, let the incident electron beam carry a polarization $\mathcal{P}_e$ but the positron beam be unpolarized. For LEP1, the incident electron beam is unpolarized ($\mathcal{P}_e = 0$), whereas for SLC one has partial polarization ($\mathcal{P}_e \simeq 0.75$).

In the following, the symbols σ_F and σ_B refer to

$$\sigma_F = 2\pi \int_0^1 d\cos\theta \, \frac{d\sigma}{d\Omega}, \qquad \sigma_B = 2\pi \int_{-1}^0 d\cos\theta \, \frac{d\sigma}{d\Omega}, \tag{2.8}$$

and σ_L, σ_R denote the cross section for an incident left-handed and right-handed polarized electron. Then three types of asymmetry are:

https://doi.org/10.1017/9781009291033.017 Published online by Cambridge University Press

$$A_{FB} \equiv \frac{\sigma_F - \sigma_B}{\sigma_F + \sigma_B} \qquad \text{[forward–backward]}, \tag{2.9a}$$

$$A_{LR} \equiv \frac{\sigma_L - \sigma_R}{\sigma_L + \sigma_R} \qquad \text{[left–right]}, \tag{2.9b}$$

$$A_{LRFB} \equiv \frac{(\sigma_F - \sigma_B)_L - (\sigma_F - \sigma_B)_R}{(\sigma_F - \sigma_B)_L + (\sigma_F - \sigma_B)_R} \qquad \text{[left–right forward-backward]}, \tag{2.9c}$$

and the relation of these to the asymmetry parameter of Eq. (2.7) is

$$A_{FB}^{(f)} = \frac{3}{4}\mathcal{A}_f \frac{\mathcal{A}_e + \mathcal{P}_e}{1 + \mathcal{A}_e\mathcal{P}_e} \qquad A_{LR} = \mathcal{A}_e\mathcal{P}_e \qquad A_{FBLR}^{(f)} = \frac{3}{4}\mathcal{A}_f. \tag{2.10}$$

Yet another approach is to exploit the fact that final-state tau leptons themselves carry a polarization $\mathcal{P}_\tau$, which affects the tau angular distribution as well as its FB asymmetry $\mathcal{P}_{FB}^{(\tau)}$. As such, the LEP1 experiments were able to extract the asymmetry parameters $\mathcal{A}_\tau$ and $\mathcal{A}_e$ via the polarization measurements

$$\mathcal{A}_\tau = -\mathcal{P}_\tau, \qquad \mathcal{A}_e = -\frac{4}{3}\mathcal{P}_{FB}^{(\tau)}. \tag{2.11}$$

The above set of asymmetries were the subject of much study for a number of years. One interesting example is the high-precision measurement of $\mathcal{A}_{LR}$ carried out by the SLD collaboration [Ab *et al.* (SLD collab.) 00]. The left–right asymmetry was measured from the e^+e^- production cross section by counting (mainly) hadronic final states for each of the two longitudinal polarizations of the incident electron beam at energies near the Z^0 mass. Despite the emphasis on detecting final-state hadrons, this measurement actually probes the asymmetry parameter of the incident-state electrons,

$$A_{LR} = \frac{1 - 4\bar{s}_\ell^2}{1 - 4\bar{s}_\ell^2 + 8\bar{s}_\ell^2}, \tag{2.12}$$

where we have assumed lepton universality in writing the weak mixing angle as $\bar{s}_\ell^2$. The precision measurement of A_{LR} then leads to the following determination of $\bar{s}_\ell^2$,

$$A_{LR}^{(e)} = 0.15138 \pm 0.00216, \qquad \bar{s}_\ell^2 = 0.23097 \pm 0.00027. \tag{2.13}$$

In summary, the collection of measurements taken at scale $\mu = M_Z$ has, on the whole, been in agreement with Standard Model expectations.

Let us conclude by commenting on just a few topics:

(1) Effective weak mixing angle $\bar{s}_\ell$: Adopting a Higgs mass value $M_H = 125$ GeV, the Standard Model prediction [ErS 13] $\bar{s}_\ell^2 = 0.23158$ is consistent with the experimental determination $\bar{s}_\ell^2 = 0.23153 \pm 0.00016$.

https://doi.org/10.1017/9781009291033.017 Published online by Cambridge University Press

(2) Unresolved issue: A long-standing item is the roughly 3σ difference between the two most precise individual measurements $\bar{s}_\ell = 0.23097 \pm 0.00027$ (via $\mathcal{A}_{LR}$ from the SLD production cross sections discussed earlier) and $\bar{s}^2_\ell = 0.23221 \pm 0.00029$ (via $\mathcal{A}_{FB}$ from the $Z^0 \to b\bar{b}$ transition found at LEP). Despite much discussion, the issue remains unresolved.

(3) Quantum corrections: The large collection of high-quality Z^0 data has provided determinations which are sensitive to quantum corrections. For example, the result $g_{\rm a}^{(\ell)} = -0.50125 \pm 0.00026$ (found in part by assuming lepton universality) implies via Eq. (2.1) that $\rho_\ell = 1.005 \pm 0.001$. This differs from the bare value $\rho_\ell^{(\rm tree)} = 1.000$ by 5σ and attests that quantum corrections have indeed been probed. Some even more impressive examples appear in Sect. I of [FeS 12].

Definitions of the weak mixing angle

Thus far in this chapter, we have made reference to three different versions of (and notations for) the weak mixing angle,

$$\text{Effective}: \ \bar{s}^2_f \qquad \text{On-shell}: \ s^2_{\rm w} \qquad \overline{\rm MS}: \ \hat{s}^2_{\rm w}(\mu). \tag{2.14}$$

Since there is, in principle, an unlimited number of renormalization prescriptions for a given quantity in quantum field theory, it is no surprise to come across the three above usages in the literature (several others, not covered here, also exist). Let us briefly consider their relation to each other, starting with the effective weak angle for a lepton ℓ.

Given the definition for $\bar{s}^2_\ell$ in Eq. (2.2b), it's clear that this quantity is tied to the ratio $\bar{g}_{\rm v}^{(\ell)}/\bar{g}_{\rm a}^{(\ell)}$ as measured at the scale $\mu = M_Z$. The motivation for doing things this way is a matter of convenience for the massive experimental effort by the Z^0 factories – one reads off a basic quantity of the Standard Model directly in terms of Z^0-related data. The current precise determination, given earlier and repeated here, of $\bar{s}^2_\ell = 0.23153 \pm 0.00016$ attests to the success achieved by the Z^0-factory experimentalists in doing precision physics.

We have already seen (cf. Sect. II–1) how modified minimal subtraction ($\overline{\rm MS}$) can be implemented in dimensional regularization for the electric charge $e(q^2)$, and one proceeds accordingly for the weak mixing angle $\hat{s}^2_{\rm w}(q^2)$ (or $s_{\rm w}(q^2)_{\overline{\rm MS}}$) by adopting the scale-dependent definition [Ma 79, MaS 81],

$$\hat{s}^2_{\rm w}\left(q^2\right) \equiv \frac{e^2\left(q^2\right)}{g_2^2\left(q^2\right)}. \tag{2.15}$$

A fit to the current database yields the value appearing already in Table XVI–1, viz., $\hat{s}^2_{\rm w}(M_Z) = 0.23125 \pm 0.00016$.

https://doi.org/10.1017/9781009291033.017 Published online by Cambridge University Press

The effective and $\overline{\rm MS}$ descriptions of the weak mixing angle can be related [GaS 94]. As pointed out in [GaS 94] there was, at the time of the LEP1 operation, 'considerable confusion among theorists and experimentalists alike as to the precise conceptual and numerical relation between the two'. The analysis in [GaS 94] established that

$$\bar{s}^2_\ell = Re\hat{\kappa}_\ell(M_Z)\,\hat{s}^2_{\rm w}(M_Z) \simeq 1.0012\,\hat{s}^2_{\rm w}(M_Z) \simeq \hat{s}^2_{\rm w}(M_Z) + 0.0003. \tag{2.16}$$

This is in accord with the individual values for $\bar{s}^2_\ell$ and $\hat{s}^2_{\rm w}(M_Z)$ given above.

Finally, the on-shell weak mixing angle is *defined* in terms of the physical gauge-boson masses,

$$s^2_{\rm w} \equiv 1 - M^2_W/M^2_Z. \tag{2.17a}$$

Thus, the on-shell weak mixing angle can be experimentally determined directly from M_W and M_Z. Inserting the gauge-boson mass values from Table I–1 into Eq. (2.17a), one has

$$s^2_{\rm w}\big|_{M_W,M_Z} = 0.2229 \pm 0.0003. \tag{2.17b}$$

The current uncertainty in $s^2_{\rm w}\big|_{M_W,M_Z}$, about twice that in $\bar{s}^2_\ell$ and $\hat{s}^2_{\rm w}(M_Z)$, is due largely to the $W^\pm$ mass uncertainty, $\delta M_W = 15$ MeV, compared to the much smaller $\delta M_Z = 2.1$ MeV. With the completion of the Tevatron data analysis, along with the resumption of LHC operations, the precision gap between the direct on-shell determination and the alternative $\bar{s}^2_\ell$ and $\hat{s}^2_{\rm w}(M_Z)$ schemes is expected to be narrowed. Even so, the fact that the on-shell scheme contains some relatively large $\mathcal{O}(G_\mu m^2_t)$ corrections (see Sect. XVI–6 for a discussion) not present in $\overline{\rm MS}$ renormalization lessens its appeal for use in electroweak perturbation theory.

Returning to the idea of scale-dependent (or running) quantities, consider the possibility of relating gauge coupling constants $\hat{g}_k$ $(k = 1, 2, 3)$ in the $\overline{\rm MS}$ scheme at the Z^0 scale with those of a 'grand unified' theory defined at an energy $E_{\rm GUT} \gg M_Z$. The so-called GUT scale signals the existence of a gauge group undergoing spontaneous symmetry breaking to $SU(3)_c \times SU(2)_L \times U(1)_Y$. The condition

$$\hat{g}_1 = \hat{g}_2 = \hat{g}_3 \qquad (E = E_{\rm GUT}) \tag{2.18}$$

leads to a prediction [GeQW 74] for the weak mixing angle at the scale $E_{\rm GUT}$. In the grand unified theory of $SU(5)$ [GeG 74, La 81] and its supersymmetric extension ($SUSY$–$SU(5)$), the $\overline{\rm MS}$ weak mixing angle obeys

$$\hat{s}^2_{\rm w}(E_{\rm GUT}) = 3/8. \tag{2.19}$$

https://doi.org/10.1017/9781009291033.017 Published online by Cambridge University Press

At the much lower energy scale $\mu = M_Z$, this value is reduced by a calculable amount,[4]

$$\hat{s}^2_{\rm w}(M_Z) \equiv \bar{s}^2_{\rm w} = \frac{3}{8}\left[1 - C\frac{\bar{\alpha}}{2\pi}\ln\frac{M_X}{M_Z} + \cdots\right], \tag{2.20}$$

where $\bar{\alpha} \equiv \hat{\alpha}(M_Z)$, M_X is the mass scale of the superheavy gauge bosons, and C is a constant which depends upon the number n_H of Higgs doublets,

$$C = \begin{cases} \dfrac{110 - n_H}{9} & (SU(5)) \\ \dfrac{30 - n_H}{3} & (SUSY\text{–}SU(5)). \end{cases} \tag{2.21}$$

The $SU(5)$ extension of the Standard Model has $n_H = 1$, whereas the minimal supersymmetric model takes $n_H = 2$.

The 'bare-bones' $SU(5)$ model turns out to be unacceptable. It is well known to give rise to an unacceptably short proton lifetime, and precision data indicate that the three coupling constants of the Standard Model *disagree* with a single unification point if evolved according to $SU(5)$ [AmBF 91]. Interestingly, the $SUSY$ extension improves matters in both respects. The rate at which $\hat{s}^2_{\rm w}(\mu)$ 'runs' is decreased due to contributions from supersymmetric partners ('sparticles') of the known particles, and the unification scale is raised to a level ($M_X \simeq 10^{16}$ GeV) consistent with the observed proton stability. The unification condition of Eq. (2.18) is better satisfied. Studies continue on whether supersymmetry breaking yields insights regarding masses of the long-sought $SUSY$ 'sparticles'.

XVI–3 Some $W^{\pm}$ properties

We shall return to issues regarding the weak mixing angle and its several definitions in Sect. XVI–4. Before that, however, we consider some aspects of $W^{\pm}$ physics. The LEP2 (e^+e^-), the Tevatron ($\bar{p}p$) and the LHC (pp), colliders have provided copious $W^{\pm}$-related data.

Decays of $W^{\pm}$ into fermions

The decay of a W-boson into a lepton and neutrino pair $\ell\nu_\ell$ is governed by the lagrangian,[5]

$$\mathcal{L}^{\rm (lept)}_{\rm ch} = -\frac{g_2}{\sqrt{8}}\, W^+_\mu \overline{\nu}_\ell \gamma^\mu (1 + \gamma_5)\ell \;+\; \text{h.c.} \tag{3.1}$$

[4] Actually, Eq. (2.20) represents a simplification in that (i) lowest-order estimates for the renormalization-group coefficients are employed, (ii) supersymmetry-breaking effects are ignored, and (iii) the fact that $m_t > M_Z$ is also ignored.

[5] Although we shall denote tree-level decay widths, cross sections, etc. with a zero superscript in this section, for the sake of notational simplicity, we shall suppress the zero subscript for bare parameters.

https://doi.org/10.1017/9781009291033.017 Published online by Cambridge University Press

It is a straightforward exercise to compute the tree-level decay width,

$$\Gamma^{(0)}_{W\to\overline{\nu}_\ell\ell} = \frac{g_2^2}{8}\frac{M_W}{6\pi}(1-x)\left(1-\frac{x}{2}-\frac{x^2}{2}\right) \underset{x\to 0}{\longrightarrow} \frac{1}{6\pi}\frac{G_\mu}{\sqrt{2}}M_W^3, \tag{3.2}$$

where $x \equiv m_\ell^2/M_W^2$ and we have employed Eq. (II–3.43). Including a small electroweak correction, we have $\Gamma_{W\to\bar{e}\nu_e} \simeq 0.226$ GeV.

There exist also decays $W \to \overline{q}^{(i)}q^{(j)}$ into quark modes (the superscripts i, $j = 1, 2, 3$ are generation labels), induced by the lagrangian

$$\mathcal{L}^{(\mathrm{qk})}_{\mathrm{ch}} = -\frac{g_2}{\sqrt{8}}\, W^+_\mu V_{ij}\, \overline{q}^{(i)}_k \gamma^\mu(1+\gamma_5) q^{(j)}_k \;+\; \mathrm{h.c.}, \tag{3.3}$$

where V_{ij} is a CKM matrix element, and the index k labels color. The lowest-order decay width for quark emission is

$$\sum_{\mathrm{color}} \Gamma^{(0)}_{W\to\overline{q}^{(i)}q^{(j)}} = \frac{1}{2\pi}\frac{G_\mu}{\sqrt{2}}M_W^3 \left|V_{ij}\right|^2 \left[1-2(x+\overline{x})+(x-\overline{x})^2\right]^{1/2} \times \left[1-\frac{x+\overline{x}}{2}-\frac{(x-\overline{x})^2}{2}\right] \underset{x,\overline{x}\to 0}{\longrightarrow} \frac{1}{2\pi}\frac{G_\mu}{\sqrt{2}}M_W^3\left|V_{ij}\right|^2, \tag{3.4}$$

where $x, \overline{x}$ are mass ratios defined as above, and we assume that all emitted quarks eventually convert to hadrons. Since the t quark is too massive to be a product of W decay, a sum over accessible quark flavors yields $\sum_{i,j}\left|V_{ij}\right|^2 = 2$. For decay into quarks, these lowest-order partial decay widths are modified by δ_{QCD}, the *QCD* factor of Eq. (2.4b) introduced in our earlier discussion of Z^0 hadronic decays.

If all final-state masses are ignored, the predicted total width for $W^\pm$ decay into fermions is

$$\Gamma^{(\mathrm{tot})}_{W^\pm} = \Gamma^{(\mathrm{had})}_{W^\pm} + \Gamma^{(\mathrm{lept})}_{W^\pm} \simeq 2.093\ \mathrm{GeV}\left(\frac{M_W(\mathrm{GeV})}{80.385}\right)^3. \tag{3.5}$$

An average of data [RPP 12] yields the value $\Gamma^{(\mathrm{tot})}_{W^\pm} = 2.085 \pm 0.042$ GeV, which is consistent with the prediction of Eq. (3.5). The current experimental uncertainty far exceeds that from theory. In the limit of massless final-state particles, the branching ratio for decay into a lepton pair $\ell\bar{\nu}_\ell$ is $(\mathrm{Br})_\ell \simeq 1/9$ ($\ell = e,\ \mu,\ \tau$), while inclusive decay to a mode containing a positively charged quark q ($q = u, c$) gives $(\mathrm{Br})_q \simeq 1/3$.

Triple-gauge couplings

The $SU(2) \times U(1)$ lagrangian of Eq. (II–3.10) and the $SU(2)$ field strength tensor of Eq. (II–3.11) alert us that there will be trilinear and quadrilinear couplings of the

https://doi.org/10.1017/9781009291033.017 Published online by Cambridge University Press

gauge bosons. We shall limit our discussion here to the so-called *charged* triple-gauge couplings (TGCs). Upon using Eq. (II–3.30) to replace the neutral gauge bosons B_μ, W^3_μ with the physical fields A_μ, Z^0_μ, we can write an effective WWV ($V = Z^0, \gamma$) lagrangian as[6]

$$\mathcal{L}_{WWV} = i g_{WWV} \left[g_1^V \left(W^\dagger_{\mu\nu} W^\mu - W_{\mu\nu} W^{\mu\dagger} \right) V^\nu + \kappa_V W^\dagger_\mu W_\nu V^{\mu\nu} + i \frac{\lambda_V}{M_W^2} W^\dagger_{\rho\mu} W^\mu_\nu V^{\nu\rho} \right], \tag{3.6a}$$

where $W_{\mu\nu} \equiv \partial_\mu W_\nu - \partial_\nu W_\mu$, $V_{\mu\nu} \equiv \partial_\mu V_\nu - \partial_\nu V_\mu$ and g_{WWV} represents the coupling strengths

$$g_{WW\gamma} = -e, \qquad g_{WWZ^0} = -e \cot\theta_{\rm w}. \tag{3.6b}$$

The above lagrangian is constrained to contain only terms which are invariant under charge-conjugation (C), parity (P), and $SU(2) \times U(1)$ gauge transformations. In the Standard Model, the individual couplings in Eq. (3.6a) become

$$g_1^V = 1, \qquad \kappa_V = 1, \qquad \lambda_V = 0 \qquad \left(V = Z^0, \gamma\right), \tag{3.6c}$$

and are consistent with the following constraint of gauge invariance,

$$\kappa_Z = g_1^Z - (\kappa_\gamma - 1) \tan^2\theta_{\rm w}, \qquad \lambda_Z = \lambda_\gamma. \tag{3.6d}$$

A recent review of LEP experiments gives [Sc *et al.* 13]

$$g_1^Z = 0.984^{+0.018}_{-0.020}, \quad \kappa_\gamma = 0.982 \pm 0.042, \quad \lambda_\gamma = -0.022 \pm 0.019, \tag{3.7}$$

consistent with Standard Model expectations.

We can read off static electromagnetic properties of the W boson upon taking $V = \gamma$. The decomposition in Eq. (3.6a) allows for the existence of a magnetic dipole moment μ_W and an electric quadrupole moment q_W,

$$\mu_W = \frac{e}{2M_W}(1 + \kappa_\gamma + \lambda_\gamma), \qquad q_W = -\frac{e}{M_W^2}(\kappa_\gamma - \lambda_\gamma), \tag{3.8a}$$

or to lowest order in the Standard Model (SM),

$$\mu_W^{\rm SM} = e/M_W, \qquad q_W^{\rm SM} = e/M_W^2. \tag{3.8b}$$

A number of experimental studies of the TGCs, especially data from the LEP2 e^+e^-, the Tevatron $\bar{p}p$, and the LHC pp colliders, has emphasized searching for *anomalous* TGCs, often expressed in terms of the five quantities,

$$\Delta g_1^Z \equiv g_1^Z - 1, \quad \Delta\kappa_Z \equiv \kappa_Z - 1, \quad \Delta\kappa_\gamma \equiv \kappa_\gamma - 1, \quad \lambda_Z, \quad \lambda_\gamma. \tag{3.9}$$

[6] Unlike TGCs with two $W^\pm$ bosons, purely neutral gauge-boson vertices are not present at tree level in the Standard Model.

https://doi.org/10.1017/9781009291033.017 Published online by Cambridge University Press

These constitute anomalous behavior in that they vanish for the Standard Model values in Eq. (3.6c). Currently, no experimental evidence exists for any of the anomalous TGCs, for example

$$\begin{aligned} -0.038 < \lambda_Z < +0.031, \qquad & -0.111 < \Delta\kappa_\gamma < 0.142 \qquad [\text{CMS}], \\ -0.074 < \lambda_Z < +0.073, \qquad & -0.135 < \Delta\kappa_\gamma < 0.190 \qquad [\text{ATLAS}]. \end{aligned} \tag{3.10}$$

The status of recent bounds is indicated by the results the LHC detectors. ATLAS and CMS will be performing further studies at higher energies and, even lacking discovery of such effects, will supply ever more stringent bounds on anomalous behavior.

We can expand the preceding discussion to incorporate possible violations of parity and charge-conjugation invariance, for which an appropriate effective lagrangian $\widetilde{\mathcal{L}}_{WWV}$ which does just this is

$$\begin{aligned} \widetilde{\mathcal{L}}_{WWV} = g_{WWV} \Bigg[& i\widetilde{\kappa}_V W^\dagger_\mu W_\nu \widetilde{V}^{\mu\nu} + i\frac{\widetilde{\lambda}_V}{M_W^2} W^\dagger_{\alpha\mu} W^\mu_\nu \widetilde{V}^{\nu\alpha} \\ & + g_4^V W^\dagger_\mu W_\nu \left(\partial^\mu V^\nu + \partial^\nu V^\mu\right) + g_5^V \epsilon^{\mu\nu\alpha\beta} \left(W^\dagger_\mu \partial_\alpha W_\nu - \partial_\alpha W^\dagger_\mu \cdot W_\nu\right) V_\beta \Bigg]. \end{aligned} \tag{3.11}$$

Here, $\widetilde{\kappa}_\gamma$ and $\widetilde{\lambda}_\gamma$ are P-violating but C-invariant, whereas g_4^V respects P but not C and g_5^V respects neither P nor C. In particular, the W boson could itself have static properties which violate at least some of the discrete symmetries. For example, an electric dipole moment d_W or magnetic quadrupole moment $\widetilde{q}_W$ would be parameterized as

$$d_W = \frac{e}{2M_W}\left(\widetilde{\kappa}_\gamma + \widetilde{\lambda}_\gamma\right), \qquad \widetilde{q}_W = -\frac{e}{M_W^2}\left(\widetilde{\kappa}_\gamma - \widetilde{\lambda}_\gamma\right). \tag{3.12}$$

Limits on the neutron electric dipole moment can be used to place a bound on the W electric dipole moment [MaQ 86], and an updated evaluation gives $|d_W| \leq 5 \times 10^{-21}$ e-cm.

XVI–4 The quantum electroweak lagrangian

In the following three sections, we shall give a simple description of how electroweak radiative corrections are calculated. We begin by quantizing the classical electroweak lagrangian to obtain certain of its Feynman rules. We also expand on earlier comments made in Sect. XVI–1 regarding on-shell renormalization.

https://doi.org/10.1017/9781009291033.017 Published online by Cambridge University Press

Classical electroweak theory of three fermion generations is defined by an $SU(2)_L \times U(1)_Y$ gauge-invariant lagrangian,[7]

$$\mathcal{L}_{\rm ew}^{\rm (cl)} = \mathcal{L}_{\rm ew}^{\rm (cl)} \left(\left\{ \psi_{L,R}^{(f)} \right\}, \mathbf{W}_\mu, B_\mu, \Phi \, ; \{g_f\}, g_1, g_2, \lambda, v^2 \right), \tag{4.1}$$

where Φ is the Higgs doublet and the collection $\{g_f\}$ of Higgs–fermion coupling constants is flavor-nondiagonal. With spontaneous symmetry breaking, all particles but the photon become massive and diagonalization of the neutral gauge-boson mass matrix occurs in the basis of the photon A_μ and massive gauge-boson Z_μ^0 fields, as given at tree level by Eq. (II–3.30). In addition, diagonalization of the charged-fermion and neutrino mass matrices for the three-generation system involves additional mixing angles and phases. The physical degrees of freedom of the gauge and Higgs sectors become manifest in unitary gauge (cf. Sect. XV–1),

$$\mathcal{L}_{\rm ew}^{\rm (cl)} = \mathcal{L}_{\rm ew}^{\rm (cl)} \left(\left\{ \psi^{(f)} \right\}, W_\mu^\pm, Z_\mu^0, A_\mu, H_0 \, ; \{m_f\}, M_W, M_Z, M_H, e \right), \tag{4.2}$$

where the fermion mixing parameters are included in the $\{m_f\}$.

Gauge fixing and ghost fields in the electroweak sector

The quantum electroweak lagrangian $\mathcal{L}_{\rm ew}^{\rm (qm)}$ will contain, in addition to the classical lagrangian of Eq. (4.1), both gauge-fixing and ghost-field contributions,

$$\mathcal{L}_{\rm ew}^{\rm (qm)} = \mathcal{L}_{\rm ew}^{\rm (cl)} + \mathcal{L}_{\rm ew}^{\rm (g\text{-}f)} + \mathcal{L}_{\rm ew}^{\rm (gh)}. \tag{4.3}$$

Mixing between gauge fields and unphysical Higgs fields occurs in the covariant derivative of the Higgs doublet (cf. Eq. (II–3.18)),[8]

$$\begin{aligned} \mathcal{L}_{HG} &= \left| \left(\mathbf{I} \left(\partial_\mu + \frac{i}{2} g_1 B_\mu \right) + \frac{i}{2} g_2 \vec{\boldsymbol{\tau}} \cdot \vec{W}_\mu \right) \Phi \right|^2 + \cdots \\ &= i \frac{g_1}{2} (\partial^\mu \Phi)^\dagger B_\mu \Phi + i \frac{g_2}{2} (\partial^\mu \Phi)^\dagger \vec{\boldsymbol{\tau}} \cdot \vec{W}_\mu \, \Phi + \text{h.c.} + \cdots . \end{aligned} \tag{4.4}$$

One can arrange the gauge-fixing term to cancel such mixing contributions. Expressing the complex Higgs doublet in terms of the physical field H_0, unphysical fields χ_+, χ_3, and the vacuum expectation value v as

$$\Phi = \frac{1}{\sqrt{2}} \begin{pmatrix} \sqrt{2}\chi_+ \\ H_0 + i\chi_3 + v \end{pmatrix}, \tag{4.5}$$

we write the gauge-fixing contribution in the form,

[7] We have replaced the Higgs parameter μ^2 by the equivalent quantity v^2.
[8] Mixing also occurs, of course, between the neutral gauge fields B_μ, W_μ^3.

https://doi.org/10.1017/9781009291033.017 Published online by Cambridge University Press

$$\mathcal{L}_{\rm ew}^{\rm (g\text{-}f)} = -\frac{1}{2\xi_+}\left|\partial_\mu W_+^\mu - \frac{\xi_+ g_2 v}{2}\chi_+\right|^2 - \frac{1}{2\xi_3}\left(\partial_\mu W_3^\mu - \frac{\xi_3 g_2 v}{2}\chi_3\right)^2 - \frac{1}{2\xi_0}\left(\partial_\mu B^\mu + \frac{\xi_0 g_1 v}{2}\chi_3\right)^2. \tag{4.6}$$

It is not hard to see that cancelation of the unwanted Higgs–gauge mixing terms occurs for arbitrary values of the gauge-fixing parameters $\xi_{+,3,0}$. Even with this cancelation, there remain in $\mathcal{L}_{\rm ew}^{\rm (g\text{-}f)}$ quadratic terms containing the unphysical Higgs fields, and such terms will contribute to the propagators of these fields.

As explained in App. A–6, once the gauge fixing is specified as in Eq. (4.6), the structure of the Faddeev–Popov lagrangian $\mathcal{L}_{\rm ew}^{\rm (gh)}$ of ghost fields is determined. For the electroweak sector, it turns out that there are four ghost fields,

$$\mathcal{L}_{\rm ew}^{\rm (gh)} = \mathcal{L}_{\rm ew}^{\rm (gh)}(\mathbf{c}_W, c_B). \tag{4.7}$$

These are associated with the four gauge fields $\mathbf{W}_\mu$, B_μ which appear in the original $SU(2)_L \times U(1)_Y$ symmetric lagrangian.

A subset of electroweak Feynman rules

The full set of electroweak Feynman rules is rather lengthy and we refer the reader to the detailed discussions in [BöHS 86, AoHKKM 82] or to the summary in [Ho 90]. A few of the more useful rules, expressed in terms of bare parameters are[9]

fermion W-boson vertex:

$$-i\,\frac{e}{2\sqrt{2}s_{\rm w}} V_{ij}\left[\gamma_\mu(1+\gamma_5)\right]_{\alpha\beta} \tag{4.8a}$$

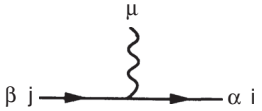

fermion Z-boson vertex:

$$-i\,\frac{e}{2s_{\rm w}c_{\rm w}}\left[\gamma_\mu(g_{\rm v}^{(f)} + g_{\rm a}^{(f)}\gamma_5)\right]_{\alpha\beta} \tag{4.8b}$$

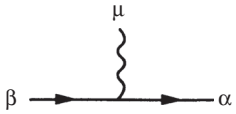

[9] For notational simplicity, we suppress the zero subscript in the following discussion.

https://doi.org/10.1017/9781009291033.017 Published online by Cambridge University Press

W-boson propagator $i\,D^{(\mathrm{W})}_{\mu\nu}(q)$:

$$\frac{i}{q^2 - M_W^2 + i\epsilon}\left[-g_{\mu\nu} + \frac{q_\mu q_\nu (1-\xi_+)}{q^2 - \xi_+ M_W^2 + i\epsilon}\right] \qquad \text{(4.8c)}$$

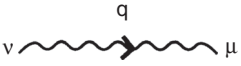

Z-boson propagator $i\,D^{(\mathrm{Z})}_{\mu\nu}(q)$:

$$\frac{i}{q^2 - M_Z^2 + i\epsilon}\left[-g_{\mu\nu} + \frac{q_\mu q_\nu (1-\xi_Z)}{q^2 - \xi_Z M_Z^2 + i\epsilon}\right] \qquad \text{(4.8d)}$$

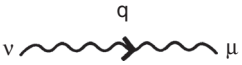

unphysical charged Higgs propagator $i\,\Delta^{(\chi_+)}(q)$:

$$\frac{i}{q^2 - \xi_+ M_W^2 + i\epsilon} \qquad \text{(4.8e)}$$

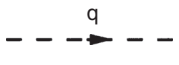

In the above, (V_{ij}) is a matrix element for quark-mixing, $g^{(f)}_{(\mathrm{v,a})}$ are given in Eq. (II–3.41), and ξ_Z is defined by expressing the gauge fixing in the form of Eq. (4.6) but using the physical neutral fields.

As seen in Eqs. (4.8c), (4.8e), each boson propagator is explicitly gauge-dependent and, in particular, the propagator of the unphysical χ_+ vanishes in the $\xi_+ \to \infty$ limit of the unitary gauge. This is as expected, because only physical degrees of freedom appear in unitary gauge. In fact, the absence of unphysical degrees of freedom in unitary gauge would appear to be an appealing reason for carrying out the computation of radiative corrections in this gauge. However, there is a 'hidden cost'. In unitary gauge, the $W^\pm$ propagator of Eq. (4.8c) becomes

$$i\,D^{(\mathrm{W})}_{\mu\nu}(q)\Big|_{\text{unitary}} = i\,\frac{-g_{\mu\nu} + q_\mu q_\nu / M_W^2}{q^2 - M_W^2 + i\epsilon}, \qquad \text{(4.9)}$$

and the high-energy behavior produced by the $q_\mu q_\nu / M_W^2$ term makes this a questionable choice for doing higher-order calculations. Instead, as the price for acceptable high-energy behavior, many opt to accept the presence of unphysical fields. One popular choice of gauge fixing is the *'t Hooft–Feynman gauge*, defined by setting all the gauge-fixing parameters equal to unity, $\xi_i = 1$. In this gauge, the lowest-order propagators for the physical gauge bosons and unphysical Higgs and ghost fields have poles at either M_W^2 or M_Z^2. This condition can be maintained in higher orders by a suitable renormalization of the gauge-fixing parameters.

https://doi.org/10.1017/9781009291033.017 Published online by Cambridge University Press

On-shell determination of electroweak parameters

The topic of electroweak radiative corrections to Standard Model quantities has been well developed over many years of research and by now there exists an impressively large literature. To focus our attention, there is one aspect that we will particularly address in the following. Given that the largest mass parameter in the Standard Model is that of the top quark, a natural question regards the effect m_t has on the set of electroweak corrections. The answer turns out to depend on the renormalization prescription followed, its effect being largest in the so-called on-shell scheme.

Two sets of electroweak parameters appear in the classical lagrangians of Eqs. (4.1), (4.2),

$$\text{classical parameter sets} = \begin{cases} \{g_f\},\, g_1,\, g_2,\, \lambda,\, v^2 & \text{(Eq. (4.1))}, \\ \{m_f\},\, M_W,\, M_Z,\, M_H,\, e & \text{(Eq. (4.2))}. \end{cases}$$

Considered as bare (input) parameters to the quantum theory, these obey the simple tree-level relations

$$\begin{aligned} M_{W,0} &= v_0 \frac{g_{2,0}}{2}, \qquad M_{Z,0} = v_0 \frac{g_{1,0}^2 + g_{2,0}^2}{2}, \qquad e_0^{-2} = g_{1,0}^{-2} + g_{2,0}^{-2}, \\ M_{H,0} &= v_0 \sqrt{2\lambda_0}, \qquad m_{f,0} = v_0 \frac{g_{f,0}}{\sqrt{2}}. \end{aligned} \tag{4.10}$$

At this stage, there are several (equivalent) expressions for the bare weak mixing angle, e.g.,

$$s_{\mathrm{w},0}^2 = 1 - \frac{M_{W,0}^2}{M_{Z,0}^2} \qquad \text{or} \qquad s_{\mathrm{w},0}^2 = \frac{g_{1,0}^2}{g_{1,0}^2 + g_{2,0}^2}. \tag{4.11}$$

The second relation becomes Eq. (2.15) in the $\overline{\mathrm{MS}}$ renormalization.

Radiative corrections will generally modify tree-level relations and, as a result, necessitate a precise definition of the weak mixing angle. Following the analysis in [Si 80], let us compare the parameter subsets $(g_{1,0},\ g_{2,0},\ v_0^2)$ and $(e_0, M_{W,0}, M_{Z,0})$. Each of these bare quantities will experience a shift,

$$\begin{aligned} g_{1,0} &= g_1 - \delta g_1, \qquad g_{2,0} = g_2 - \delta g_2, \qquad v_0^2 = v^2 - \delta v^2, \\ e_0 &= e - \delta e, \qquad M_{W,0}^2 = M_W^2 + \delta M_W^2, \qquad M_{Z,0}^2 = M_Z^2 + \delta M_Z^2. \end{aligned} \tag{4.12}$$

In on-shell renormalization, the theory is specified in terms of e, M_W, and M_Z. Moreover, the following relations are arranged to hold order by order,

$$e^{-2} = g_1^{-2} + g_2^{-2}, \qquad M_W^2 = v^2 \frac{g_2^2}{4}, \qquad M_Z^2 = v^2 \frac{\left(g_1^2 + g_2^2\right)}{4}. \tag{4.13}$$

These equations constrain the effects of radiative corrections upon the parameters.

https://doi.org/10.1017/9781009291033.017 Published online by Cambridge University Press

By differentiating the three relations in Eq. (4.13), one finds after a modest amount of algebra the conditions,

$$\begin{pmatrix} \frac{\delta g_1^2}{g_1^2} \\ \frac{\delta g_2^2}{g_2^2} \\ \frac{\delta v^2}{v^2} \end{pmatrix} = \begin{pmatrix} -1 & 1 & 1 \\ \frac{c_{\rm w}^2}{s_{\rm w}^2} & -\frac{c_{\rm w}^2}{s_{\rm w}^2} & 1 \\ \frac{s_{\rm w}^2 - c_{\rm w}^2}{s_{\rm w}^2} & \frac{c_{\rm w}^2}{s_{\rm w}^2} & -1 \end{pmatrix} \begin{pmatrix} \frac{\delta M_W^2}{M_W^2} \\ \frac{\delta M_Z^2}{M_Z^2} \\ \frac{\delta e^2}{e^2} \end{pmatrix}. \tag{4.14}$$

Also in on-shell renormalization, one *defines* the weak mixing angle in terms of the masses M_W, M_Z as in Eq. (2.17a). Since this relation is to be maintained to all orders, the bare value $s_{\rm w,0}^2$ will be modified by shifts in the W and Z masses,

$$\begin{aligned} s_{\rm w,0}^2 &= 1 - \frac{M_{W,0}^2}{M_{Z,0}^2} = 1 - \frac{M_W^2 + \delta M_W^2}{M_Z^2 + \delta M_Z^2} \\ &\simeq s_{\rm w}^2 \left[1 - \cot^2\theta_{\rm w} \left(\frac{\delta M_W^2}{M_W^2} - \frac{\delta M_Z^2}{M_Z^2} \right) \right]. \end{aligned} \tag{4.15}$$

For any renormalizable field theory, it makes sense to express results in terms of the most accurately measured quantities available. Thus, it is preferable in the electroweak sector to replace M_W by G_μ and work with a modified parameter set,

$$\text{Physical parameter set} = \begin{cases} \alpha^{-1} = 137.035999173(35), \\ G_\mu = 1.1663787(6) \times 10^{-5}\ \text{GeV}^{-2}, \\ M_Z = 91.1876(21)\ \text{GeV}. \end{cases} \tag{4.16}$$

To accomplish this, the relationship $G_\mu = G_\mu(\alpha, M_W, M_Z, \dots)$ can be used to replace M_W by G_μ.

XVI–5 Self-energies of the massive gauge bosons

It is is evident from Eq. (4.14) that the parameter shifts δe^2, δM_W^2 and δM_Z^2 play an important role in the study of electroweak radiative corrections. We have already determined from our analysis of *QED* (cf. Eq. (II–1.30)) that

$$\frac{\delta e^2}{e^2} = -\Pi(0), \tag{5.1}$$

where the photon vacuum polarization $\Pi(q^2)$ appears in Eq. (II–1.26). In this section, we shall compute the portion of δM_W^2 and δM_Z^2 arising from the fermionic vacuum polarization contributions to the $W^\pm$ and Z^0 propagators. As a consequence, we shall be able to reveal the presence of propagator contributions which scale as $\mathcal{O}(G_\mu m_t^2)$.

https://doi.org/10.1017/9781009291033.017 Published online by Cambridge University Press

The charged gauge bosons $W^{\pm}$

The radiative correction experienced by a $W^{\pm}$ gauge boson propagating at momentum q is expressed in terms of a self-energy function, $\Pi^{\mu\nu}_{\rm ww}(q^2)$,

$$\Pi^{\mu\nu}_{\rm ww}\left(q^2\right) \equiv A_{\rm ww}\left(q^2\right) g^{\mu\nu} - B_{\rm ww}\left(q^2\right) q^{\mu} q^{\nu}. \tag{5.2}$$

(For notational simplicity in this subsection we denote W and Z boson subscripts for the quantities $\Pi^{\mu\nu}$, A, and B in terms of lower-case Roman indices.) Although a vector-boson propagator $i D_{\mu\nu}(q)$ generally contains terms proportional to $g_{\mu\nu}$ and to $q_\mu q_\nu$, it will suffice to study just the $g_{\mu\nu}$ part. As indicated at the end of Sect. II–3, the $q_\mu q_\nu$ dependence is absent if the gauge boson couples to a conserved current or will give rise to suppressed contributions if the external particles have small mass. Thus, we have for the W propagator in 't Hooft–Feynman gauge,

$$\begin{aligned}
\frac{-i g_{\mu\nu}}{q^2 - M^2_{W,0}} &\to \frac{-i g_{\mu\nu}}{q^2 - M^2_{W,0}} + \frac{-i g_{\mu\alpha}}{q^2 - M^2_{W,0}} \left(-i A_{\rm ww}(q^2) g^{\alpha\beta}\right) \frac{-i g_{\beta\nu}}{q^2 - M^2_{W,0}} \\
&\to \frac{-i g_{\mu\nu}}{q^2 - M^2_{W,0} + A_{\rm ww}(q^2)} \\
&= \frac{-i g_{\mu\nu}}{q^2 - M^2_W + A_{\rm ww}(q^2) - \delta M^2_W},
\end{aligned} \tag{5.3}$$

where we have substituted for the bare W mass using Eq. (4.12).

Let us now calculate the loop contribution of a fermion–antifermion pair $f_1 \bar{f}_2$ to the self-energy $A_{\rm ww}(q^2)$. We begin with

$$\begin{aligned}
-i \Pi^{\alpha\beta}_{\rm ww}(q^2)\Big|_{f_1\bar{f}_2} &= -\frac{(-i g_2)^2 \eta_{f_1\bar{f}_2}}{8} \\
&\quad \times \int \frac{d^4 p}{(2\pi)^4} \,{\rm Tr}\, \left[\gamma^{\alpha}(1+\gamma_5) \frac{i}{\not{p} - m_1} \gamma^{\beta}(1+\gamma_5) \frac{i}{\not{p} - \not{q} - m_2}\right],
\end{aligned} \tag{5.4}$$

where $\eta_{f_1\bar{f}_2} = N_c |V_{f_1 f_2}|^2$ for the case when the fermions are quarks. Aside from the occurrence of the $1+\gamma_5$ chiral factor and the nondegeneracy in fermion masses m_1, m_2, the above Feynman integral is identical to the photon vacuum polarization function of Eq. (II–1.20). It is thus straightforward to evaluate this quantity in dimensional regularization, and we find for the $g^{\alpha\beta}$ component,

https://doi.org/10.1017/9781009291033.017 Published online by Cambridge University Press

$$A_{\rm ww}^{(f_1\bar{f}_2)}(q^2) = \frac{\eta_{f_1\bar{f}_2} g_2^2}{24\pi^2}\left[q^2\left\{\frac{2}{\epsilon} - \frac{\gamma}{2} + \ln\sqrt{4\pi}\right.\right.$$
$$\left. -3\int_0^1 dx\; x(1-x)\ln\frac{M^2 - q^2x(1-x)}{\mu^2}\right\}$$
$$\left. -\frac{3}{2}\left\{(m_1^2+m_2^2)\left[\frac{2}{\epsilon} - \frac{\gamma}{2} + \ln\sqrt{4\pi}\right] - \int_0^1 dx\; M^2\ln\frac{M^2 - q^2x(1-x)}{\mu^2}\right\}\right], \tag{5.5}$$

where $M^2 \equiv m_1^2 x + m_2^2(1-x)$. Since the $W^\pm$ boson is an unstable particle with decay rate Γ_W, the function $A_{\rm ww}(q^2)$ is complex-valued, and we consider its real and imaginary parts separately.

From Eq. (5.5), we see that Re $A_{\rm ww}(q^2)$ is divergent. One can construct a finite quantity $\hat{A}_{\rm ww}(q^2)$ by defining the field renormalization, $\mathbf{W}_{\mu,0} = (Z_2^W)^{1/2}\mathbf{W}_\mu$, and constraining δM_W^2 and δZ_2^W to cancel the ultraviolet divergence in Re $A_{\rm ww}(q^2)$,

$$\hat{A}_{\rm ww}\left(q^2\right) \equiv A_{\rm ww}\left(q^2\right) - \delta M_W^2 + \delta Z_2^W\left(q^2 - M_W^2\right). \tag{5.6}$$

It follows from Eq. (5.6) that the mass shift δM_W^2 is fixed by

$$\delta M_W^2 = \text{Re } A_{\rm ww}\left(M_W^2\right), \tag{5.7}$$

and the $f_1\bar{f}_2$ contribution to the field renormalization, which ensures that $\hat{A}_{\rm ww}(M_W^2) = 0$ is

$$\delta Z_2^W[f_1\bar{f}_2] = \frac{\eta_{f_1\bar{f}_2} g_2^2}{8\pi^2}\left[\frac{2}{\epsilon} - \frac{\gamma}{2} + \ln\sqrt{4\pi}\right]. \tag{5.8}$$

To obtain a relation for the imaginary part of the self-energy, we recall that instability in a propagating state of mass M is described by the replacement $M \to M - i\Gamma/2$. This produces the following modification of a propagator denominator,

$$\frac{1}{q^2 - M^2} \to \frac{1}{q^2 - M^2 + iM\Gamma}, \tag{5.9}$$

where we ignore the $\mathcal{O}(\Gamma^2)$ term. Comparison with Eq. (5.5) then immediately yields

$$\text{Im } A_{\rm ww}(M_W^2) = M_W\Gamma_W. \tag{5.10}$$

We can use Eq. (5.6) to check this relation by setting $q^2 = M_W^2$. If, for simplicity, we neglect the masses of the fermion–antifermion pair $f_1\bar{f}_2$, then the imaginary part comes from the logarithm contained in the first of the integrals in Eq. (5.5),

$$\text{Im}\int_0^1 dx\; x(1-x)\ln\frac{-q^2x(1-x)}{\mu^2 - i\epsilon} \underset{q^2=M_W^2}{\longrightarrow} -\frac{\pi}{6}, \tag{5.11}$$

https://doi.org/10.1017/9781009291033.017 Published online by Cambridge University Press

and we obtain

$$\Gamma_{W\to f_1\bar{f}_2} = \frac{\mathrm{Im}\left[A_{ww}^{(f_1\bar{f}_2)}\left(M_W^2\right)\right]}{M_W} = \eta_{f_1\bar{f}_2}\frac{G_\mu M_W^3}{6\sqrt{2}\pi}, \tag{5.12}$$

where we have substituted $g_2^2 = 4\sqrt{2}M_W^2 G_\mu$. This agrees with the results of our earlier decay width calculations for W decay in Sect. XVI–3.

The neutral gauge bosons Z^0, γ

The system of neutral gauge bosons is treated analogously to the charged case except that we must deal with a 2×2 propagator matrix, and the issue of particle mixing arises. Although the neutral channel was already diagonalized at tree level (cf. Eq. (II–3.30)), interactions reintroduce nondiagonal propagator contributions at higher orders. The $g_{\mu\nu}$ part of the neutral channel inverse propagator $\mathbf{D}^{-1}_{[\mathrm{ntl}]\mu\nu}\left(q^2\right)$, diagonal at tree level,

$$\mathbf{D}^{(0)-1}_{[\mathrm{ntl}]\mu\nu}\left(q^2\right) = ig_{\mu\nu}\begin{pmatrix} q^2 & 0 \\ 0 & q^2 - M_{Z,0}^2 \end{pmatrix}, \tag{5.13}$$

has the renormalized form,

$$\mathbf{D}^{(0)-1}_{[\mathrm{ntl}]\mu\nu}\left(q^2\right) \to \mathbf{D}^{-1}_{[\mathrm{ntl}]\mu\nu}\left(q^2\right) = g_{\mu\nu}\begin{pmatrix} q^2 + \hat{A}_{\gamma\gamma}\left(q^2\right) & \hat{A}_{\gamma z}\left(q^2\right) \\ \hat{A}_{\gamma z}\left(q^2\right) & q^2 - M_Z^2 + \hat{A}_{zz}\left(q^2\right) \end{pmatrix}. \tag{5.14}$$

Upon taking the inverse, we obtain for the individual neutral boson renormalized propagators,

$$\begin{aligned} D^{\mu\nu}_{\gamma\gamma}\left(q^2\right) &= \frac{-ig^{\mu\nu}}{q^2 + \hat{A}_{\gamma\gamma}\left(q^2\right) - \hat{A}^2_{\gamma z}\left(q^2\right) / \left(q^2 - M_Z^2 + \hat{A}^2_{zz}\left(q^2\right)\right)}, \\ D^{\mu\nu}_{zz}\left(q^2\right) &= \frac{-ig^{\mu\nu}}{q^2 - M_Z^2 + \hat{A}_{zz}\left(q^2\right) - \hat{A}^2_{\gamma z}\left(q^2\right) / \left(q^2 + \hat{A}^2_{\gamma\gamma}\left(q^2\right)\right)}, \\ D^{\mu\nu}_{\gamma z}\left(q^2\right) &= \frac{ig^{\mu\nu}\hat{A}_{\gamma z}\left(q^2\right)}{\left[q^2 + \hat{A}_{\gamma\gamma}\left(q^2\right)\right]\left[q^2 - M_Z^2 + \hat{A}^2_{\gamma\gamma}\left(q^2\right)\right] - \hat{A}^2_{\gamma z}\left(q^2\right)}. \end{aligned} \tag{5.15}$$

Observe that there is indeed a particle-mixing propagator, $D^{\mu\nu}_{\gamma z}$, proportional to the the reduced self-energy $\hat{A}_{\gamma z}(q^2)$. It might appear from Eq. (5.15) that Z^0-photon mixing gives rise to a photon mass contribution. However, one arranges as a renormalization condition that $\hat{A}_{\gamma z}(0) = 0$, and the photon remains massless under electroweak radiative corrections.

https://doi.org/10.1017/9781009291033.017 Published online by Cambridge University Press

If we consider only the vacuum-polarization loop contribution due to a fermion of mass m, we obtain for the Z^0 self-energy,

$$-i\Pi_{zz}^{\alpha\beta}\left(q^2\right) = N_c\left(\frac{ig_2}{2c_w}\right)^2 \int \frac{d^4p}{(2\pi)^4}\frac{N^{\alpha\beta}}{\left(p^2-m^2\right)\left((p-q)^2-m^2\right)}, \tag{5.16}$$

where m is the fermion mass, N_c is a quark color factor, and

$$\begin{aligned} N^{\alpha\beta} = {} & g_v^{(f)2}\,\mathrm{Tr}\,\left[\gamma^\alpha \not{p}\gamma^\beta(\not{p}-\not{q}) + m^2\gamma^\alpha\gamma^\beta\right] \\ & + g_a^{(f)2}\,\mathrm{Tr}\,\left[\gamma^\alpha \not{p}\gamma^\beta(\not{p}-\not{q}) - m^2\gamma^\alpha\gamma^\beta\right]. \end{aligned} \tag{5.17}$$

The quantities in $N^{\alpha\beta}$ are just those expected from the coupling of fermion f to the neutral weak current. We then obtain, using dimensional regularization,

$$\begin{aligned} A_{zz}^{(f\bar{f})}(q^2) = \frac{g_2^2 N_c}{16\pi^2 c_w^2}\Bigg[& \frac{2q^2(g_v^{(f)2}+g_a^{(f)2})}{3}\left\{\frac{2}{\epsilon}-\frac{\gamma}{2}+\ln\sqrt{4\pi}\right. \\ & \left. -3\int_0^1 dx\; x(1-x)\ln\frac{m^2-q^2x(1-x)}{\mu^2}\right\} \\ & +4m^2 g_a^{(f)2}\left\{\frac{2}{\epsilon}-\frac{\gamma}{2}+\ln\sqrt{4\pi}-\frac{1}{2}\int_0^1 dx\;\ln\frac{m^2-q^2x(1-x)}{\mu^2}\right\}\Bigg]. \end{aligned} \tag{5.18}$$

It is also easy to demonstrate that the photon–Z^0 self-energy $A_{\gamma z}^{(f\bar{f})}$ is proportional to $A_{\gamma\gamma}^{(f\bar{f})}$ for the case of a charged-fermion loop contribution,

$$A_{\gamma z}^{(f\bar{f})}\left(q^2\right) = \frac{g_v^{(f)}}{2c_w s_w Q_f} A_{\gamma\gamma}^{(f\bar{f})}\left(q^2\right), \tag{5.19}$$

where Q_f is the electric charge of the fermion.

XVI–6 Examples of electroweak radiative corrections

All electroweak amplitudes will be affected by radiative corrections. We have already pointed out our interest in potentially large contributions arising from the heavy masses m_t and M_H. We shall find leading corrections which are quadratic in the top-quark mass ($\mathcal{O}(G_\mu m_t^2)$).[10] To begin this section, we consider corrections to the coefficients ρ_f and κ_f of Eq. (1.5), followed by an analysis of the quantum correction known as Δr, and finally the $Z \to b\bar{b}$ vertex correction. A historical overview of electroweak corrections appears in [FeS 12], and a thorough state-of-the-art presentation is given by Erler and Langacker in [RPP 12].

[10] Recall from Chap. XV that corrections at leading order are only logarithmic in the Higgs mass ($\mathcal{O}(\ln[M_H^2/M_Z^2])$).

https://doi.org/10.1017/9781009291033.017 Published online by Cambridge University Press

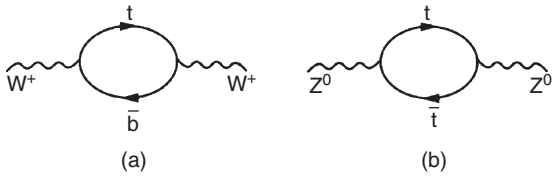

Fig. XVI–3 Top-quark corrections to the (a) $W^{\pm}$, (b) Z^0 propagators.

The $\mathcal{O}(G_\mu m_t^2)$ contribution to Δ_ρ

Contributions to ρ_f and κ_f can be classified as either independent of the external fermions (*universal*) or explicitly dependent on the fermion flavor f (*nonuniversal*). Recalling that at tree level these quantities reduce to unity, we have

$$\rho_f = 1 + \Delta\rho + (\Delta\rho)^{(f)}_{\text{nonuniv}}, \qquad \kappa_f = 1 + \Delta\kappa + (\Delta\kappa)^{(f)}_{\text{nonuniv}}, \tag{6.1}$$

where $\Delta\rho$ and $\Delta\kappa$ denote universal pieces. It should be apparent that $W^{\pm}$- and Z^0-propagator corrections, like those in Fig. XVI–3, occur independent of the external fermions and are thus 'universal'. Nonuniversal effects have been found to be small (i.e. subdominant) except for the $Z^0 \to \bar{b}b$ vertex. The universal effects are of special interest because they turn out to be the primary source of $\mathcal{O}(G_\mu m_t^2)$ radiative corrections [Ve 77*a*, ChFH 78]. As such, in the following we shall approximate

$$\Delta\rho = (\Delta\rho)_t + \cdots, \qquad \Delta\kappa = \frac{c_{\text{w}}^2}{s_{\text{w}}^2}(\Delta\rho)_t + \cdots, \tag{6.2}$$

where

$$(\Delta\rho)_t = \frac{3G_\mu m_t^2}{8\pi^2\sqrt{2}} \simeq 0.00942 \times \left(\frac{m_t}{173.4\ \text{GeV}}\right)^2. \tag{6.3}$$

Observe in Eq. (6.2) that $\Delta\kappa$ is proportional to $\Delta\rho$. This is a result of the Standard Model; in general, these quantities are independent.

The quantity $\Delta\rho$ can be defined as a correction to the rho parameter of Eq. (1.3),

$$\begin{aligned} \rho_0 &= \frac{1}{c_{\text{w},0}^2} \cdot \frac{D_Z(q^2=0)}{D_W(q^2=0)} \\ \rho_0 + \Delta\rho &= \frac{M_Z^2 + \delta M_Z^2}{M_W^2 + \delta M_W^2} \cdot \frac{\left(-M_Z^2 - \delta M_Z^2 + A_{\text{zz}}(0)\right)^{-1}}{\left(-M_W^2 - \delta M_W^2 + A_{\text{ww}}(0)\right)^{-1}} \end{aligned} \tag{6.4}$$

or

$$\Delta\rho = \frac{A_{\text{zz}}(0)}{M_Z^2} - \frac{A_{\text{ww}}(0)}{M_W^2}. \tag{6.5}$$

https://doi.org/10.1017/9781009291033.017 Published online by Cambridge University Press

Observe that $\Delta\rho$ is finite since the singular terms in Eqs. (5.5), (5.18) cancel. If we set $m_1 = m_t$ and $m_2 = m_b$ in Eq. (5.5) and include both t-quark and b-quark loops in Eq. (5.18), a simple calculation reveals that $\Delta\rho = 0$ in the limit that $m_t = m_b$. However, the leading term in the small m_b limit gives

$$(\Delta\rho)_t = \frac{g_2^2 N_c}{16\pi^2 M_W^2} \int_0^1 dx \left[\frac{m_t^2}{2} \ln \frac{m_t^2}{\mu^2} - x m_t^2 \ln \frac{x m_t^2}{\mu^2} \right] + \cdots$$
$$= \frac{g_2^2 N_c}{64\pi^2} \frac{m_t^2}{M_W^2} + \cdots . \tag{6.6}$$

Substitution of $N_c = 3$ and $G_\mu/\sqrt{2} = g_2^2/8M_W^2$ yields the result shown in Eqs. (6.2), (6.3).

This quadratic dependence on the heavy-top-quark mass is in striking contrast with the behavior observed for the photon self-energy (cf. Eq. (II–1.26)). In the heavy-fermion limit, the photon vacuum polarization exhibits instead the decoupling result $\mathcal{O}(m_t^{-2})$. The reason for this difference is that *QED* is a vector theory, whereas the charged and neutral weak interactions are chiral. Indeed, one can show (cf. Prob. XVI–2) that the decoupling expected of a vector interaction results when left-handed and right-handed self-energies are averaged. However, equally important is the fact that as m_t grows while m_b is kept fixed, the weak doublet is being split in mass. Thus, decoupling of the top quark in the large m_t limit should not be expected because if we were to integrate out the top quark, we would no longer have a renormalizable theory – the remaining low-energy theory would have an incomplete weak doublet. Early contributions to this subject appear in [Ve 77*b*] and [ChFH 78]. As noted above, if both members of the doublet are taken to be *equally* heavy ($m_t = m_b \to \infty$), there would exist no quadratic dependence on the heavy-quark mass, and the decoupling theorem (cf. Sect. IV–2) would be satisfied. It is the large splitting in the weak doublet which leads to the observable violation of decoupling.

Even though two different renormalization schemes must give the same final set of results, intermediate details will generally differ. For example, the leading m_t behaviors for the coefficients ρ_f and κ_f of Eq. (1.5) are [RPP 12],

$$\begin{aligned} &\text{on-shell}: \quad \rho_f \sim 1 + (\Delta\rho)_t + \cdots \qquad && \kappa_f \sim 1 + \frac{c_{\rm w}^2}{s_{\rm w}^2}(\Delta\rho)_t + \cdots \\ &\overline{\text{(MS)}}: \quad \hat{\rho}_f \sim 1 + \cdots && \hat{\kappa}_f \sim 1 + \cdots , \end{aligned} \tag{6.7}$$

where $(\Delta\rho)_t$ is defined in Eq. (6.3).[11]

[11] The case $f = b$ is special; the leading behaviors are $\hat{\rho}_f \sim 1 - 4(\Delta\rho)_t/3$ and $\hat{\kappa}_f \sim 1 + 2(\Delta\rho)_t/3$.

https://doi.org/10.1017/9781009291033.017 Published online by Cambridge University Press

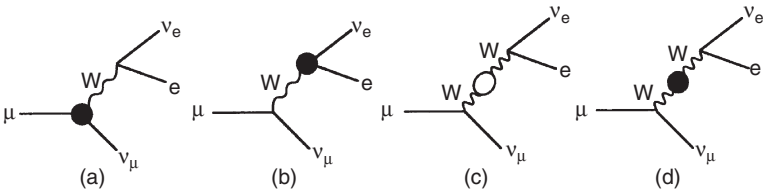

Fig. XVI–4 (a)–(b) Vertex, (c) propagator, and (d) mass-shift counterterm corrections to muon decay.

The $\mathcal{O}(G_\mu m_t^2)$ contribution to Δr

The quantity Δr describes the effect of electroweak corrections on the leading order relation which defines the muon decay constant. In particular, the tree-level relation of Eq. (II–3.43) becomes modified by the radiative corrections of Fig. XVI–4 [Si 80, BuJ 89],

$$\frac{G_{\mu,0}}{\sqrt{2}} = \frac{g_{2,0}^2}{8M_{W,0}^2} \quad \rightarrow \quad \frac{G_\mu}{\sqrt{2}} = \frac{g_2^2}{8M_W^2}[1+\Delta r]. \tag{6.8a}$$

It is to be understood in Eq. (6.8a) that 'G_μ' is determined from the muon lifetime with the photonic corrections described in Sect. V–2 already taken into account. Thus, Δr contains only the remaining electroweak effects.

To trace the origin of the quantum correction, we observe first the effect of the $W^\pm$ self-energy on the bare relation in Eq. (6.8a),

$$\frac{G_\mu}{\sqrt{2}} = -\frac{g_{2,0}^2}{8}\frac{1}{q^2 - M_{W,0}^2 + A_{\rm ww}(0)} \simeq \frac{g_{2,0}^2}{8M_{W,0}^2}\left[1 + \frac{A_{\rm ww}(0)}{M_W^2} + \cdots\right], \tag{6.8b}$$

where we have taken $q^2 \simeq 0$. Next, we replace the bare parameters $g_{2,0}^2$ and $M_{W,0}^2$ by their physical forms as in Eq. (4.12). Comparison with Eq. (6.8a) directly yields

$$\Delta r = \frac{\delta M_W^2 - A_{\rm ww}(0)}{M_W^2} - \frac{\delta g_2^2}{g_2^2}. \tag{6.9}$$

Upon using Eq. (4.14) for δg_2^2, we can rewrite Eq. (6.9) as

$$\Delta r = -\frac{\delta e^2}{e^2} - \frac{c_{\rm w}^2}{s_{\rm w}^2}\left[\frac{\delta M_Z^2}{M_Z^2} - \frac{\delta M_W^2}{M_W^2}\right] + \frac{A_{\rm ww}(0) - \delta M_W^2}{M_W^2}. \tag{6.10}$$

Recalling that the $W^\pm$ and Z^0 mass shifts can be related to the self-energy functions $A_{\rm ww}(M_W^2)$ and $A_{\rm zz}(M_Z^2)$, it should be clear that Eq. (6.9) expresses Δr entirely in terms of calculable quantities.[12] Although each of the terms in Eq. (6.10) is

[12] There are additional radiative corrections, such as the 'box' diagrams, which we shall not discuss.

https://doi.org/10.1017/9781009291033.017 Published online by Cambridge University Press

divergent, the overall combination is finite. A number of rearrangements and algebraic steps can be used to isolate the leading contributions, and one finds

$$\Delta r = \Delta\alpha + \Delta r_{\rm w} + (\Delta r)_{\rm rem}, \tag{6.11}$$

where

$$\Delta\alpha \equiv \frac{\alpha\left(M_Z^2\right) - \alpha}{\alpha} \simeq \hat{\Pi}\left(M_Z^2\right), \quad \text{and} \quad \Delta r_{\rm w} = -\frac{c_{\rm w}^2}{s_{\rm w}^2}\Delta\rho. \tag{6.12}$$

$\Delta\rho$ is given by Eqs. (6.5)–(6.6), and $(\Delta r)_{\rm rem}$ contains smaller finite contributions.

The largest contribution to Δr is $\Delta\alpha$, the shift in the fine-structure constant. Although we have previously expressed the variation in $\alpha(q^2)$ in terms of fermion masses (cf. Eq. (II–1.38)), the difficulty in precisely determining quark masses would appear to undermine an accurate evaluation of $\Delta\alpha$. However, one can use dispersion relations to relate the hadronic contribution to the vacuum polarization, $\hat{\Pi}_{\rm had}(q^2)$, directly to cross-section data. Recalling Prob. V–2, we have

$$\begin{aligned}\Pi_{\rm had}^{\mu\nu}(q^2) &= ie^2 \int d^4x\, e^{iq\cdot x}\langle 0|T\left(J_{\rm em}^{\mu}(x)J_{\rm em}^{\nu}(0)\right)|0\rangle \\ &= \left(q^\mu q^\nu - q^2 g^{\mu\nu}\right)\Pi_{\rm had}\left(q^2\right).\end{aligned} \tag{6.13}$$

The imaginary part of $\Pi_{\rm had}(q^2)$ is expressible in terms of cross-section data evaluated at invariant energy q^2,

$$\text{Im}\,\Pi_{\rm had}\left(q^2\right) = \frac{\alpha}{3}\text{R}\left(q^2\right) \quad \text{with} \quad \text{R}\left(q^2\right) \equiv \frac{\sigma(e\bar{e} \to \text{hadrons})}{\sigma(e\bar{e} \to \mu\bar{\mu})}. \tag{6.14}$$

Thus, we obtain a dispersion relation for the subtracted quantity $\hat{\Pi}_{\rm had}(q^2)$,

$$\begin{aligned}\hat{\Pi}_{\rm had}\left(q^2\right) &\equiv \Pi_{\rm had}\left(q^2\right) - \Pi_{\rm had}(0) \\ &= \frac{\alpha q^2}{3\pi}\left[\int_{4m_\pi^2}^{s_0} + \int_{s_0}^{\infty}\right] ds\, \frac{\text{R}(s)}{s(s - q^2 - i\epsilon)},\end{aligned} \tag{6.15}$$

where s_0 denotes the point at which data become unavailable. For energies above s_0, a perturbative representation is used to approximate $\text{R}(s)$. The result of Eq. (6.15), when added to the lepton contributions, implies a value for $\alpha^{-1}(M_Z^2)$ [DaHMZ 11],[13]

$$\alpha^{-1}\left(M_Z^2\right) = 128.952 \pm 0.014. \tag{6.16}$$

Some feeling for the magnitudes of 'Δr' corrections is given in the following (the numerical values have been taken from [KuMMS 13]):

[13] There are minor differences in various evaluations cited in the literature, depending on how the perturbative estimate is performed or on the particular renormalization scheme.

https://doi.org/10.1017/9781009291033.017 Published online by Cambridge University Press

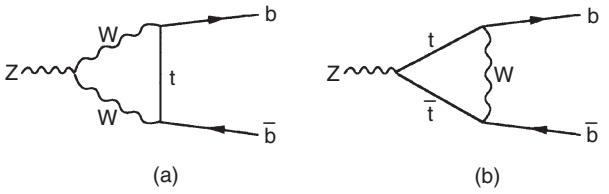

Fig. XVI–5 Top-quark corrections to the $Z^0 b\bar{b}$ vertex.

$$\begin{aligned}
\Delta r &= 1 - \frac{\pi\alpha}{\sqrt{2}G_\mu M_W^2\left(1 - M_W^2/M_Z^2\right)} = 0.0350(9),\\
\Delta\hat{r}_{\rm w} &= 1 - \frac{\pi\alpha}{\sqrt{2}G_\mu M_W^2 \hat{S}_{\rm w}^2(M_Z)} = 0.0699(7)(4),\\
\Delta\hat{r} &= 1 - \frac{\pi\alpha}{\sqrt{2}G_\mu M_Z^2 \hat{C}_{\rm w}^2(M_Z)\hat{S}_{\rm w}^2(M_Z)} = 0.0598(4).
\end{aligned} \tag{6.17}$$

The above relations, although exact at tree level (the '$\Delta r = 0$' limit), lead to the different values shown away from this limit. As before in this chapter, the quantities $\hat{s}_{\rm w}^2(M_Z)$ and $\hat{c}_{\rm w}^2(M_Z)$ are defined in $\overline{\rm MS}$ renormalization and evaluated at scale M_Z. In order to obtain the above form for Δr, we have replaced $[1 + \Delta r]$ in Eq. (6.8a) by $1/[1 - \Delta r]$, which is valid in our first-order analysis.

The $Z \to b\bar{b}$ vertex correction

The preceding analyses of $\Delta\rho$ and Δr could very well be carried out for any other electroweak observable. In most cases, we would again find important $\mathcal{O}(G_\mu m_t^2)$ radiative corrections. Thus, for example, the Z^0 width for decay into lepton ℓ ($\ell = e, \mu, \tau$) has the form

$$\Gamma_{Z^0\to\ell\bar{\ell}} = \Gamma^{(0)}_{Z^0\to\ell\bar{\ell}}\left[1 + (\Delta\rho)_t + \cdots\right], \tag{6.18}$$

and grows quadratically with increasing m_t [AkBYR 86]. The origin of this effect, the one-loop $t\bar{t}$ contribution to the Z^0 propagator, is identical to that discussed earlier.

Interestingly, however, a more complete calculation reveals a slight *decrease* to occur in the decay rate $\Gamma_{Z^0\to b\bar{b}}$ as m_t grows. This is because, although the decay amplitude contains a (universal) propagator contribution proportional to $(\Delta\rho)_t$, an even larger effect, the vertex correction of Fig. XVI–5, contributes with opposite sign [AkBYR 86, DjKZ 90],[14]

[14] Due to cancelations, the vertex correction turns out not to affect asymmetry phenomena, such as the b-quark forward–backward asymmetry $A_{FB}^{(b)}$.

https://doi.org/10.1017/9781009291033.017 Published online by Cambridge University Press

$$\Gamma_{Z^0\to b\bar{b}} = \Gamma^{(0)}_{Z^0\to b\bar{b}}\left[1 + \frac{19}{13}\left((\Delta\rho)_t + \left(\Delta v^{(b)}\right)_t\right) + \cdots\right], \tag{6.19}$$

where the $Z^0 b\bar{b}$ vertex correction is given by

$$(\Delta v^{(b)})_t = -\frac{20}{19}(\Delta\rho)_t - \frac{130}{57}\frac{\alpha}{\pi}\ln\frac{m_t^2}{M_Z^2}. \tag{6.20}$$

The $d\bar{d}, s\bar{s}$ modes also contain virtual t-quark vertex corrections, but they are greatly suppressed by the tiny accompanying CKM factors $|V_{ti}|^2$ $(i = d, s)$. Recalling the characterization given in Sect. XVI–1 of radiative corrections as either 'universal' or 'nonuniversal', one may interpet the $Z^0 b\bar{b}$ effect as a nonuniversal term which contributes as

$$(\Delta\rho)^{(b)}_{\text{nonuniv}} = -2(\Delta\kappa)^{(b)}_{\text{nonuniv}} = -\frac{4}{3}\Delta\rho - \frac{\alpha}{4\pi s_{\text{w}}^2}\left(\frac{8}{3} + \frac{1}{6c_{\text{w}}^2}\right)\ln\frac{m_t^2}{M_W^2}. \tag{6.21}$$

Although $\mathcal{O}(m_t^2)$ corrections are the most important, $\mathcal{O}(\ln(m_t^2/M_Z^2)$ logarithmic dependence has been included in Eq. (6.20) because it has a nonnegligible numerical impact.

Precision tests and New Physics

In precision electroweak tests, about 20 (mainly $W^\pm$ or Z^0) observables are fit to Standard Model predictions (e.g. see [Ba *et al.* (Gfitter group) 12, RPP 12]). Such tests are based on the availability of high-quality data (with precision at the 1% level or better), multi-loop theoretical Standard Model predictions, and sophisticated software packages.[15] In view of the LHC discovery regarding the Higgs boson, the list of detected Standard Model particles is now complete. Consequently, there will be, more than ever, an emphasis on using precision tests to probe contributions from beyond the Standard Model.

As was noted ever since the first electroweak corrections were calculated (e.g. [Ve 77*a*]), physics associated with a large-energy scale Λ should affect the gauge-boson self-energies $-i\,\Pi^i_{\mu\nu}(q)$ $(i = \gamma\gamma, \gamma z, WW, ZZ)$. In particular, the $-i\,\Pi^i_{\mu\nu}(q)$ could contain loop corrections (sometimes referred to as *oblique* corrections) from

[15] Let us describe just a few of these. The Zfitter collaboration, begun in 1985 ([AkARR 13]), established a FORTRAN library of Standard Model predictions for $e^+e^- \to \bar{f}f(+\gamma's)$ at energies $\sqrt{s} = 20 \to 150$ GeV using the on-shell renormalization scheme. The LEP electroweak working group LEPEWWG was founded in 1993 to perform fits of LEP and Tevatron data, particularly of Z-pole observables such as the effective weak mixing angle $\bar{s}_f^2$ of Eqs. (2.2b),(2.14), using Zfitter in part as input. A more recent effort using on-shell renormalization to perform electroweak global fits is the Gfitter group. The Global Analysis of Particle Properties (GAPP) software is employed by the Particle Data Group [Er 00]. This is a special purpose FORTRAN package, which performs calculations and fitting procedures and utilizes $\overline{\text{MS}}$ renormalization, Finally, the Heavy Flavor Averaging Group provides updates to world averages of heavy-flavor quantities.

https://doi.org/10.1017/9781009291033.017 Published online by Cambridge University Press

'new' particles. For $\Lambda^2 \gg q^2$, one would expect rapid convergence of an expansion for $-i\,\Pi^i_{\mu\nu}(q)$ in powers of q^2/Λ^2, yielding the following effective low-energy description,

$$-i\,\Pi^i_{\mu\nu}(q) = g_{\mu\nu}\left(A_i + q^2 A'_i\right) + \cdots . \tag{6.22}$$

This description involves eight free parameters, $A_{\gamma\gamma}, \ldots, A'_{zz}$. However, the conditions $\Pi_{\gamma\gamma}(0) = \Pi_{\gamma z}(0) = 0$ reduce this number to six. An additional three parameters can be absorbed into the renormalization of α, G_μ, M_Z, which experience the shifts [BaFGH 90],

$$\frac{\delta\alpha}{\alpha} = -A'_{\gamma\gamma}, \quad \frac{\delta G_\mu}{G_\mu} = A_{ww}, \quad \frac{\delta M_Z^2}{M_Z^2} = -\frac{A_{zz}}{M_Z^2} - A'_{zz}. \tag{6.23}$$

The three remaining parameters may be chosen to be quantities known as S, T, U and defined as [PeT 90] (we employ $\overline{\text{MS}}$ renormalization here [RPP 12])

$$\begin{aligned}
\frac{\hat\alpha\,(M_Z)}{4\hat s_Z^2\hat c_Z^2} S &\equiv \left[\frac{A_{zz}^{(\text{NP})}\left(M_Z^2\right) - A_{zz}^{(\text{NP})}(0)}{M_Z^2} - \frac{\hat c_Z^2 - \hat s_Z^2}{\hat s_Z^2\hat c_Z^2}\frac{A_{z\gamma}^{(\text{NP})}(0)}{M_Z^2} - \frac{A_{\gamma\gamma}^{(\text{NP})}(0)}{M_Z^2}\right], \\
\hat\alpha(M_Z) T &\equiv \left[\frac{A_{ww}^{(\text{NP})}(0)}{M_W^2} - \frac{A_{zz}^{(\text{NP})}(0)}{M_Z^2}\right], \\
\frac{\hat\alpha(M_Z)}{4\hat s_Z^2}(S+U) &\equiv \left[\frac{A_{ww}^{(\text{NP})}\left(M_W^2\right) - A_{ww}^{(\text{NP})}(0)}{M_W^2} - \frac{\hat c_Z}{\hat s_Z}\frac{A_{z\gamma}^{(\text{NP})}(0)}{M_Z^2} - \frac{A_{\gamma\gamma}^{(\text{NP})}(0)}{M_Z^2}\right],
\end{aligned} \tag{6.24}$$

where the superscript (NP) refers to contributions only from New Physics. Clearly, these S, T, U parameters are defined so as to vanish in the limit of only Standard Model physics. If nonzero, they would appear as new contributions to various observables, e.g.,

$$\begin{aligned}
\left[\frac{M_Z^{(\text{expt})}}{M_Z^{(\text{SM})}}\right]^2 &= \frac{1 - \hat\alpha(M_Z)T}{1 - G_\mu M_Z^{(\text{SM})2} S/(2\sqrt{2}\pi)}, \\
\left[\frac{M_W^{(\text{expt})}}{M_W^{(\text{SM})}}\right]^2 &= \frac{1}{1 - G_\mu M_W^{(\text{SM})2}(S+U)/(2\sqrt{2}\pi)}, \\
\left[\frac{M_Z^{(\text{SM})}}{M_Z^{(\text{expt})}}\right]^3 \cdot \frac{\Gamma_Z^{(\text{expt})}}{\Gamma_Z^{(\text{SM})}} &= \frac{1}{1 - \hat\alpha(M_Z)T},
\end{aligned} \tag{6.25}$$

all of which compare the experimental value with the Standard Model (SM) prediction. In this way, bounds are placed on the New Physics parameters and the results found in [RPP 12] are[16]

[16] The range of Higgs-boson masses $115.5 < M_H(\text{GeV}) < 127$ was used as input.

https://doi.org/10.1017/9781009291033.017 Published online by Cambridge University Press

$$S = 0.00^{+0.11}_{-0.10}, \qquad T = 0.02^{+0.11}_{-0,12}, \qquad U = 0.08 \pm 0.11, \tag{6.26}$$

and are consistent with Standard Model expectations. At present, the precision electroweak fits do not yet display evidence for effects beyond those predicted by the Standard Model.

The literature contains several other possible New Physics parameterizations. For example, if the scale of New Physics is not much larger than the Standard Model weak scale, then parameters X, Y, V, W will, in principle, contribute to the fitting procedure [BuGKLM 94, BaPRS 04]. However, their determination requires data at energies higher than the scale set by the Z-boson mass and so, e.g., in the work of [Ba *et al.* (Gfitter group) 12], the quantities X, Y, V, W are set equal to zero.

As we have emphasized throughout this book (e.g. Sect. IV–9), the effects of heavy particles can be analyzed theoretically by using effective lagrangians and the preceding analysis can be expressed naturally in this language (e.g. see [Sk 10]). These must respect the $SU(2)_L \times U(1)_Y$ gauge symmetry, but may or may not include the extra custodial $SU(2)_L \times SU(2)_R$ invariance of the Higgs sector with doublet Higgs fields. There will be a tower of such operators, beginning with those of dimension-six. However, not all dimension-six operators are relevant to electroweak phenomenology. Examples of these are $\left(H^\dagger H\right)^3$ and $H^\dagger H \mathcal{D}_\mu H^\dagger \mathcal{D}^\mu H$, the point being that processes having Higgs bosons as external states are presently experimentally inaccessible. Instead, we consider the two operators.[17]

$$\mathcal{O}_S \equiv H^\dagger \boldsymbol{\sigma}_i H F^i_{\mu\nu} B^{\mu\nu}, \qquad \mathcal{O}_T \equiv \left|H^\dagger \mathcal{D}_\mu H\right|^2, \tag{6.27}$$

where $B^{\mu\nu}$, $F^i_{\mu\nu}$ are, respectively, the field strength tensors defined in Eqs. (II–3.11), (II–3.12). These operators, together with the usual Standard Model lagrangian $\mathcal{L}_{\rm SM}$, can be added together to form

$$\mathcal{L} = \mathcal{L}_{\rm SM} + a_S \mathcal{O}_S + a_T \mathcal{O}_T. \tag{6.28}$$

The New Physics coefficients a_S and a_T will each carry units of inverse squared-energy and the Higgs fields in Eq. (6.27) will each contribute a factor of the symmetry-breaking energy v, so that in this approach the S, T parameters will obey

$$S \propto a_S \, v^2, \qquad T \propto a_T \, v^2, \tag{6.29}$$

and we leave evaluation of the proportionality factors to an exercise at the end of the chapter. Although we do not survey New Physics models in this book, a large variety is discussed in [Sk 10, RPP 12, Ba *et al.* 12], among others.

[17] It turns out that associated with the parameter U will be a dimension-eight operator.

https://doi.org/10.1017/9781009291033.017 Published online by Cambridge University Press

Problems

(1) **Tree-level coefficients in effective lagrangians**

(a) Using the simplest quark–parton description of protons and neutrons as uud and ddu composites, reproduce the content of the tree-level expressions of Eq. (1.7) by determining the quantities $R_{\nu,0}$ and $R_{\bar{\nu},0}$ for scattering from an isoscalar target. It might be helpful to first refer to a summary of parton phenomenology, e.g., as in [RPP 12], for guidance. Suppose a neutrino deep-inelastic experiment reports $R_\nu = 0.3072 \pm 0.0032$. Infer from this a central value and an error estimate for the tree-level quantity $s^2_{\mathrm{w},0}$.

(b) Likewise, reproduce the tree-level expressions for the coefficients $C^{(u,d)}_{1,0}$ of Eq. (1.11), and infer a value for $s^2_{\mathrm{w},0}$ assuming the value $Q_\mathrm{w} = -69.4 \pm 1.55 \pm 3.8$ for the weak nuclear charge.

(2) **Power-law radiative corrections**

(a) Verify the statement that if $m_t = m_b \to \infty$, there is no quadratic mass dependence in the calculation of $\Delta\rho$.

(b) From the combination of Dirac matrices appearing in Eq. (5.4), it is evident that the self-energy amplitude has a 'left–left' (LL) chiral structure. To see how this affects the result, repeat the analysis of Eqs. (5.4), (5.5) except now employing a 'left–right' (LR) chiral structure.

(c) By averaging the LL and LR self-energies and passing to the limit $m_1 = m_2 \to m$, reproduce the $g^{\alpha\beta}$ part of the photon self-energy of Eq. (II–1.26).

(d) If we had a purely left-handed $U(1)$ theory, the vacuum polarization would grow with m_t^2 as $m_t \to \infty$. How can this be consistent with the decoupling theorem?

(3) **Effective field theory and the *S*,*T* parameters**

Determine the proportionality factors which were not provided in Eq. (6.29).

https://doi.org/10.1017/9781009291033.017 Published online by Cambridge University Press